Electronic Supplementary Information

for

Is Silver a Mere Terminal Oxidant in Palladium Catalyzed C-H Bond Activation Reactions?

Bangaru Bhaskararao,[a] Sukriti Singh,[a] Megha Anand,[b] Pritha Verma,[a] Prafull Prakash,[a] Athira C,[a] Santanu Malakar,[a] Henry F. Schaefer,[b] and Raghavan B. Sunoj*,[a]

[a]*Department of Chemistry, Indian Institute of Technology Bombay, Powai, Mumbai 400076, India*

and

[b]*Center for Computational Quantum Chemistry, University of Georgia, Athens, GA 30602, USA*

corresponding author: sunoj@chem.iitb.ac.in

PART-A

Table of Contents

Section 1
Additional Computational Details

1.1. Computational Methods

Computations were performed using Gaussian09 suite of quantum chemical program.[1] The geometries were optimized in the condensed phase using the Cramer−Truhlar SMD continuum solvation model that employs quantum mechanical charge densities of solutes with the M06 hybrid density functional theory.[2] Pople's 6-31G** basis set were used for all atoms except for the heavy atoms. Los Alamos pseudopotential (LANL2DZ) basis set consisting of an effective core potential (ECP) for '*n*' core electrons and a double-ζ quality valence basis set for '*v*' valence electrons was employed, where (*n*,*v*) for various heavy atoms in the current study are Pd(28,18), Ag(28,19), Br(28,7) and I(46,7).[3] All the stationary points were characterized, as minima or a first-order saddle point (transition states) by evaluating the corresponding Hessian indices. The transition states were verified by examining whether it has a unique imaginary frequency representing the desired reaction coordinate. Intrinsic reaction coordinate (IRC) calculations were additionally carried out to further ascertain the true nature of the transition states in that it connects to the reactants and products.[4] The geometries obtained as the end-

[1] Frisch, M. J.; Trucks, G. W.; Schlegel, H. B.; Scuseria, G. E.; Robb, M. A.; Cheeseman, J. R.; Scalmani, G.; Barone, V.; Mennucci, B.; Petersson, G. A.; Nakatsuji, H.; Caricato, M.; Li, X.; Hratchian, H. P.; Izmaylov, A. F.; Bloino, J.; Zheng, G.; Sonnenberg, J. L.; Hada, M.; Ehara, M.; Toyota, K.; Fukuda, R.; Hasegawa, J.; Ishida, M.; Nakajima, T.; Honda, Y.; Kitao, O.; Nakai, H.; Vreven, T.; Montgomery, J. A., Jr.; Peralta, J. E.;Ogliaro, F.; Bearpark, M.; Heyd, J. J.; Brothers, E.; Kudin, K. N.; Staroverov, V. N.; Kobayashi, R.; Normand, J.; Raghavachari, K.; Rendell, A.; Burant, J. C.; Iyengar, S. S.; Tomasi, J.; Cossi, M.; Rega, N.; Millam, N. J.; Klene, M.; Knox, J. E.; Cross, J. B.; Bakken, V.; Adamo, C.; Jaramillo, J.; Gomperts, R.; Stratmann, R. E.; Yazyev, O.; Austin, A. J.; Cammi, R.; Pomelli, C.; Ochterski, J. W.; Martin, R. L.; Morokuma, K.; Zakrzewski, V. G.; Voth, G. A.; Salvador, P.; Dannenberg, J. J.; Dapprich, S.; Daniels, A. D.; Farkas, Ö.; Foresman, J. B.; Ortiz, J. V.; Cioslowski, J.; Fox, D. J. Gaussian 09, Revision A.02; Gaussian, Inc.: Wallingford, CT, 2013.

[2] Y. Zhao, D. G. Truhlar, The M06 Suite of Density Functionals for Main Group Thermochemistry, Thermochemical Kinetics, Noncovalent Interactions, Excited States, and Transition Elements: Two New Functionals and Systematic Testing of Four M06-Class Functionals and 12 Other Functionals. *Theor. Chem. Acc.* **120**, 215-241 (2008).

[3] Wadt, W. R.; Hay, P. J. Ab initio Effective Core Potentials for Molecular Calculations. Potentials for Main group Elements Na to Bi. *J. Chem. Phys.* **82**, 284-298 (1985).

[4] Gonzalez, C.; Schlegel, H. B. Reaction Path Following in Mass-Weighted Internal Coordinates. *J. Phys. Chem.* **94**, 5523-5527 (1990).

points on either side of the IRC trajectories were subjected to further optimization using a more stringent criteria "opt = calcfc" (as implemented in Gaussian09 program). This exercise enabled us to obtain the reactant and product such that their connection to the transition state could be established. Single-point energies were calculated at the SMD(solvent)/M06/6-31G**,LANL2TZ(f)(Pd,Ag),LANL2DZ(d,p)(Br,I) levels of theory using the SMD(Solvent)/M06/6-31G**,LANL2DZ(Pd,Ag,I,Br) geometries using an ultrafine integration grid. The zero-point vibrational energy (ZPVE), thermal, and entropic corrections obtained at 298.15 K and 1 atm pressure derived from the SMD(solvent)/M06/6-31G**,LANL2DZ (Pd,Ag,I,Br) level of theory have been applied to the "bottom-of-the-well" energies obtained through the single-point energy evaluations in the solvent phase at the M06 functional to estimate the Gibbs free energies of solutes in the condensed phase. The discussions in the text are presented using the Gibbs free energies thus obtained using the DFT(M06) functional in a suitable continuum solvent. Although M06 functional is generally known to yield good estimates of the energetics, we note that the trimerization energy of $[Pd(OAc)_2]_3$ was reported to be overestimated.[5] For example, the parent palladium acetate catalyst is known to exist as a trimeric species in aprotic solvents of low polarity.[4] Hence, we have considered the energy of $Pd_3(OAc)_6$ as the native species in this study. When a monomeric palladium acetate is involved, one third energy of the trimer is used in the computation of energies. Similarly, silver salts are coordinatively saturated with appropriate ligands/solvent molecules in all the reactions considered in this study. Graphical representation of the optimized geometries is created by using CYLView.[6]

1.2. Natural Bond Orbital (NBO) Analysis

The analysis of a molecular wave function is done by the NBO program[7] to identify the localized electron-pair 'bonding' units such as core (CR), bond orbital (BD), lone pairs (LP) and

---

[5] Giri, R.; Lan, Y.; Liu, P.; Houk, K. N.; Yu, J.-Q. Understanding Reactivity and Stereoselectivity in Palladium-Catalyzed Diastereoselective sp^3 C–H Bond Activation: Intermediate Characterization and Computational Studies. *J. Am. Chem. Soc*. **134**, 14118-14126 (2012).

[6] C. Y. Legault, CYLview, 1.0b, Université de Sherbrooke, Quebec (Canada), 2009, (http ://www.cylview.org)

[7] E. D. Glendening, A. E. Reed, J. E. Carpenter and F. Weinhold, *The NBO 3.0 program manual*.

the corresponding unoccupied counterparts as BD* and LP*. The Natural Population Analysis (NPA) is done using the NBOs, thus obtained. Of importance, is the second order perturbative energies ($E^{(2)}$) that is proportional to the 'donor-acceptor' interactions between the NBOs. For each donor NBO and acceptor NBO, the stabilization energy $E^{(2)}$ is associated with the delocalization or "*2e*-stabilization". The energy analysis is carried out by examining all possible interactions between 'filled' (donor) Lewis-type NBOs and 'empty' (acceptor) non-Lewis NBOs. Since these interactions lead to loss of occupancy from the localized NBOs of the idealized Lewis structure into the empty non-Lewis orbital, they are referred to as 'delocalization' corrections to the zeroth-order natural Lewis structure.

1.3. Atoms In Molecule (AIM) Analysis

Bader's theory of "Atoms in Molecules" has offered a valuable tool to analyze the nature of chemical bonds and interatomic interactions. Electron densities at the bond critical points ρ_{bcp} (a point along the bond path at the interatomic surface, where the shared electron density reaches a minimum) are calculated by using electronic wave function of the system.[8] Along with ρ, and its Laplacian ($\nabla^2\rho$), we have calculated other topological properties such as the potential electron energy density (V), the kinetic electron energy density (G), and the total electron energy density (H) at those important BCPs. By using these parameters, we analyzed the nature of interatomic interaction between Pd and Ag metals.[9]

Initially, we have evaluated AIM properties of an experimentally reported heterobimetallic Pd-Ag crystal structure.[10] The wave function of this molecule was generated by using the geometry as seen in the crystal structure. AIM properties were then evaluated using this wave function. We have compared the ρ and $\nabla^2\rho$ values for this crystal structure with all the transition states of CMD and RE steps to ascertain the presence of Pd-Ag interaction. It shows a similar trend to what we have found in the crystal structure. All wave functions of transition states are generated using the $SMD_{(solvent)}$/M06/6-31G**,LANL2DZ(Pd,Ag,Br,I) level of theory.

---

[8] (a) R. F. W. Bader, *Atoms in Molecules: A Quantum Theory*, Oxford University Press, New York, 1990; (b) R. F. W. Bader, *Chem. Rev.* 1991, **91**, 893-928.
[9] J. S. Grabowski, *Chem. Rev.* 2011, **111**, 2597-2625.
[10] N. Y. Kozitsyna, S. E. Nefedov, A. P. Klyagina, A. A. Markov, Z. V. Dobrokhotova, Y. A. Velikodny,D. I. Kochubey, T. S. Zyubina, A. E. Gekhman, M. N. Vargaftik and I. I. Moiseev, *Inorganica Chimica Acta* 2011, **370**, 373-382.

1.4. Computation of Relative Gibbs Free Energies

The energies of the transition states are computed with respect to the infinitely separated reactants.[11] Depending on the nature of the intermediates or transition states, the reactants include palladium acetate, silver salt, the substrates and other additives as appropriate. The primary catalyst, palladium acetate, is known to exist as trimeric $Pd_3(OAc)_6$ species in several solvents employed in the reactions examined in this work.[12] This prompted us to consider a more realistic trimeric palladium acetate as the reference point. When a monomeric palladium acetate is involved in any of the stationary points, the energy is deduced from the energy of the trimeric $Pd_3(OAc)_6$ as one third the energy of the trimer. Similarly, solid state crystallographic structure of silver acetate suggests a polymeric $[Ag_2(OAc)_2]_n$ species.[13] In reaction **2**, the dimeric *t*-amyl alcohol bound silver acetate $[Ag_2(OAc)_2]$.2(*t*-amyl alcohol) has been used as the reference point. In reaction **2**, the monomeric acetic acid bound silver acetate [Ag(OAc)].2(AcOH) has been used as the reference point. In reaction **3**, the analogous dimeric form $[Ag_2(OTf)_2]$ has been used as the reference.[14] In Reaction **4**, the silver salt $[Ag_2(OAc)_2]$.2(DMF) has been used as the reference.

---

[11] (a) P. Ball, *Nature* 2011, **469**, 26; (b) V. R. Jensen, K. Angermund and P. W. Jolly, *Organometallics* 2000, **19**, 403-410. c) B. Huang, L. Zhuang, L. Xiao and J. Lu, *Chem. Sci.* 2013, **4**, 606-611.

[12] (a) A. C. Skapski and M. L. Smart, *J. Chem. Soc. D* 1970, **11**, 685-686; (b) Adrio, L. A., Nguyen, B. N., Guilera, G., Livingston, A. G. and K. K. Hii, *Catal. Sci. Technol.* 2012, **2**, 316-323.

[13] L. P. Olson and D. R. Whitcomb, M. Rajeswaran, T. N. Blanton and B. J. Stwertka, B. J. *Chem. Mater.* 2006, **18**, 1667-1674.

[14] W. Grochala, M. K. Cyrański, M. Derszi, T. Michałowski, P. J. Malinowski, Z. Mazej, D. Kurzydłowski, W. Koźmiński, A. Budzianowski and P. J. Leszczyński, *Dalton Trans.* 2012, **41**, 2034-2043.

Section 2

Details of Individual Reactions, Reaction Conditions, and their Mechanism

The reactions given below can be chemically classified as phosphorylation (**1**),[15] arylation (**2**),[16] alkynylation (**3**),[17] and oxidative cycloaddition (**4**).[18] A broad overview of the heterobimetallic pathway (denoted as **2(A)**) is provided in this section. We have focused on the CMD and RE steps (shown respectively in blue and red color insets)

Reaction 1

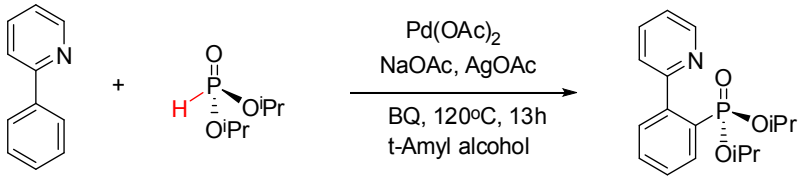

Oxidant	Additive	Yield
AgOAc	NaOAc	96 %
-	-	not reported

Reaction 2

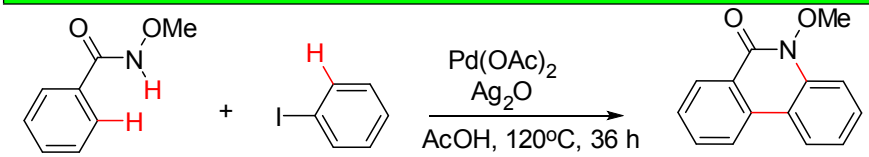

Oxidant	Yield
Ag_2O	76 %

---

[15]Feng, C. –G.; Ye, M.; Xiao, K. –J.; Li, S.; Yu, J. –Q. Pd(II)-Catalyzed Phosphorylation of Aryl C–H Bonds. *J. Am. Chem. Soc.* **135**, 9322-9325 (2013).
[16]Wang, G. -W.; Yuan, T. –T.; Li, D. –D. One-Pot Formation of C-C and C-N Bonds through Palladium-Catalyzed Dual C-H Activation: Synthesis of Phenanthridinones. *Angew. Chem. Int. Ed.* **50**, 1380-1383 (2011).
[17]Tobisu, M.; Ano, Y.; Chatani, N. Palladium-Catalyzed Direct Alkynylation of C−H Bonds in Benzenes. *Org. Lett.* **11**, 3250-3252 (2009).
[18]Wang, L.; Huang, J.; Peng, S.; Liu, H.; Jiang, X.; Wang, J. Palladium-Catalyzed Oxidative Cycloaddition through C-H/N-H Activation: Access to Benzazepines. *Angew. Chem. Int. Ed.* **52**, 1768-1772 (2013).

-	Not reported

Reaction 3

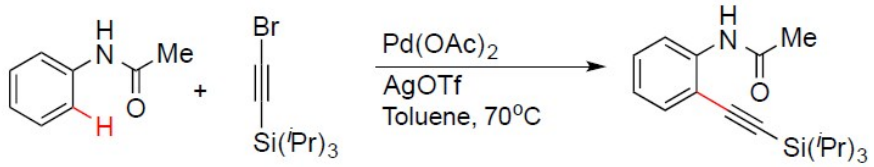

Oxidant	Additive	Yield
-	K_2CO_3	0 %
AgOTf	K_2CO_3	96 %

Reaction 4

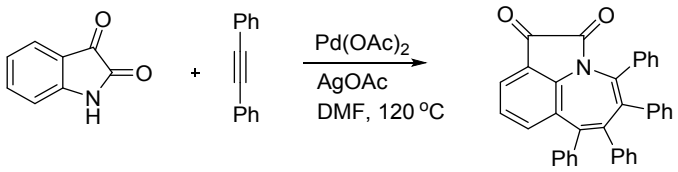

Oxidant	Yield
-	<5 %
AgOAc	77 %

2(A): Heterobimetallic Pathway

Reaction 1

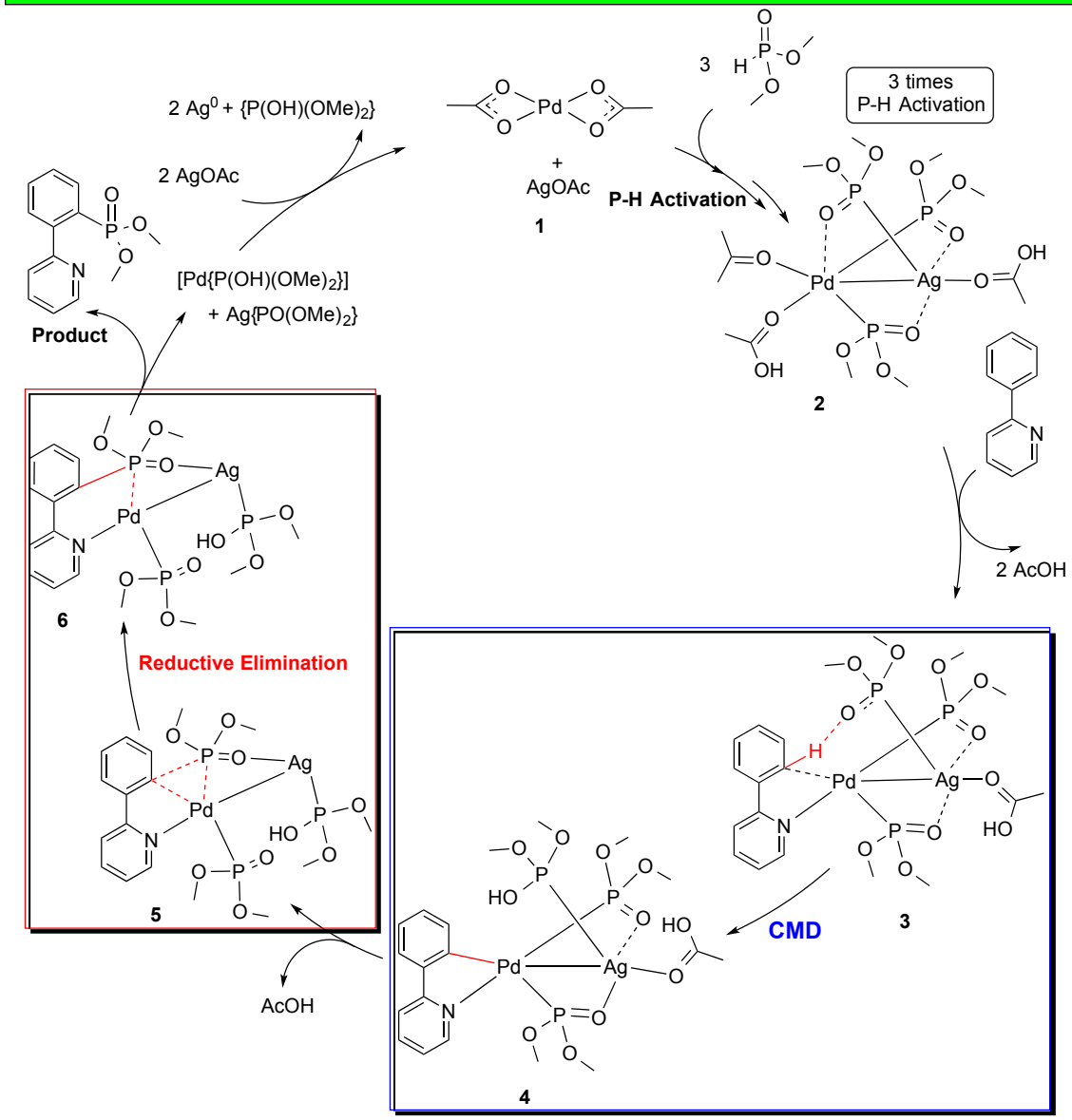

Reaction 2

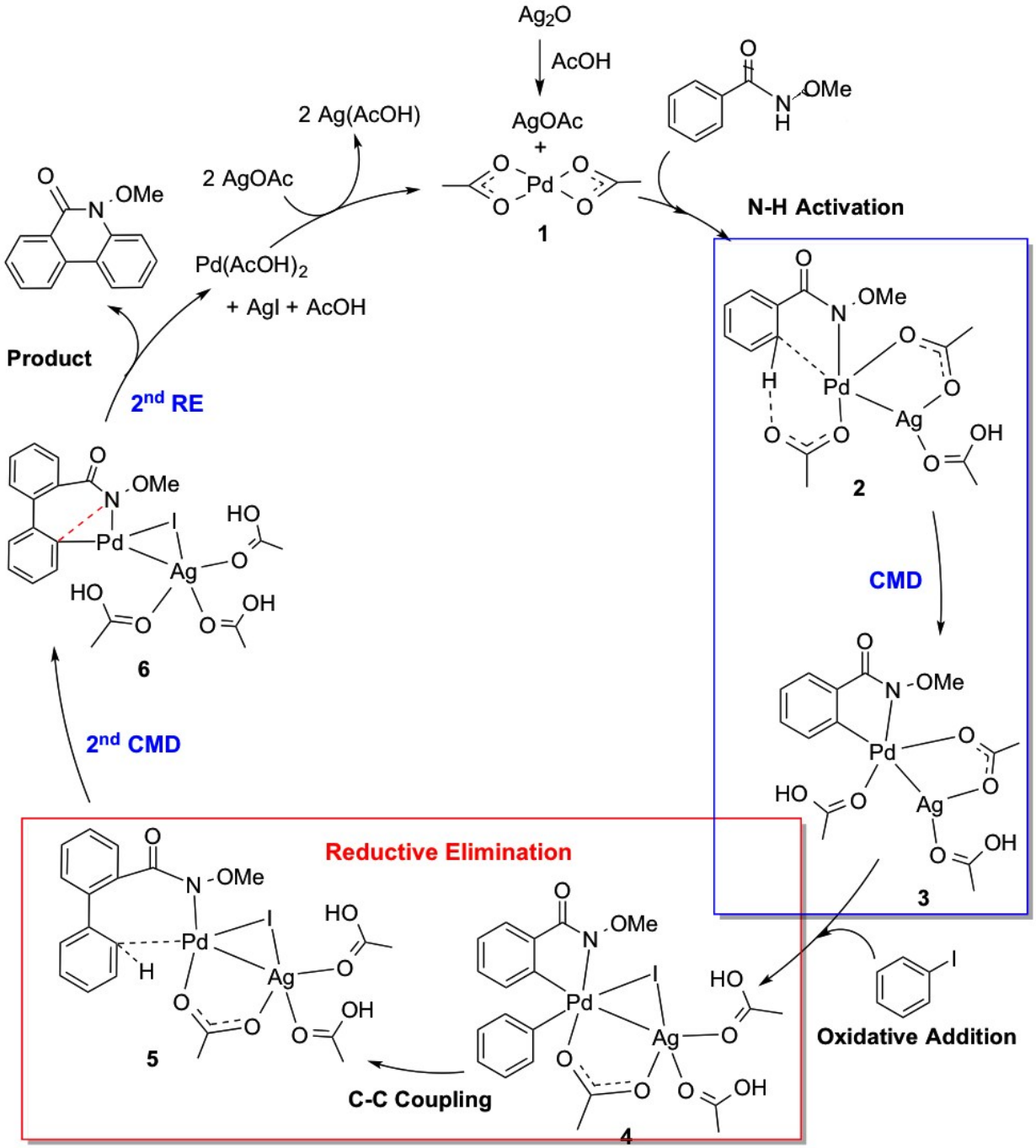
Ag2O
AcOH
AgOAc
+
2 Ag(AcOH)
2 AgOAc
Pd(AcOH)2
+ AgI + AcOH
1
N-H Activation
2
CMD
3
Oxidative Addition
4
C-C Coupling
5
Reductive Elimination
6
2nd CMD
2nd RE
Product

Reaction 3

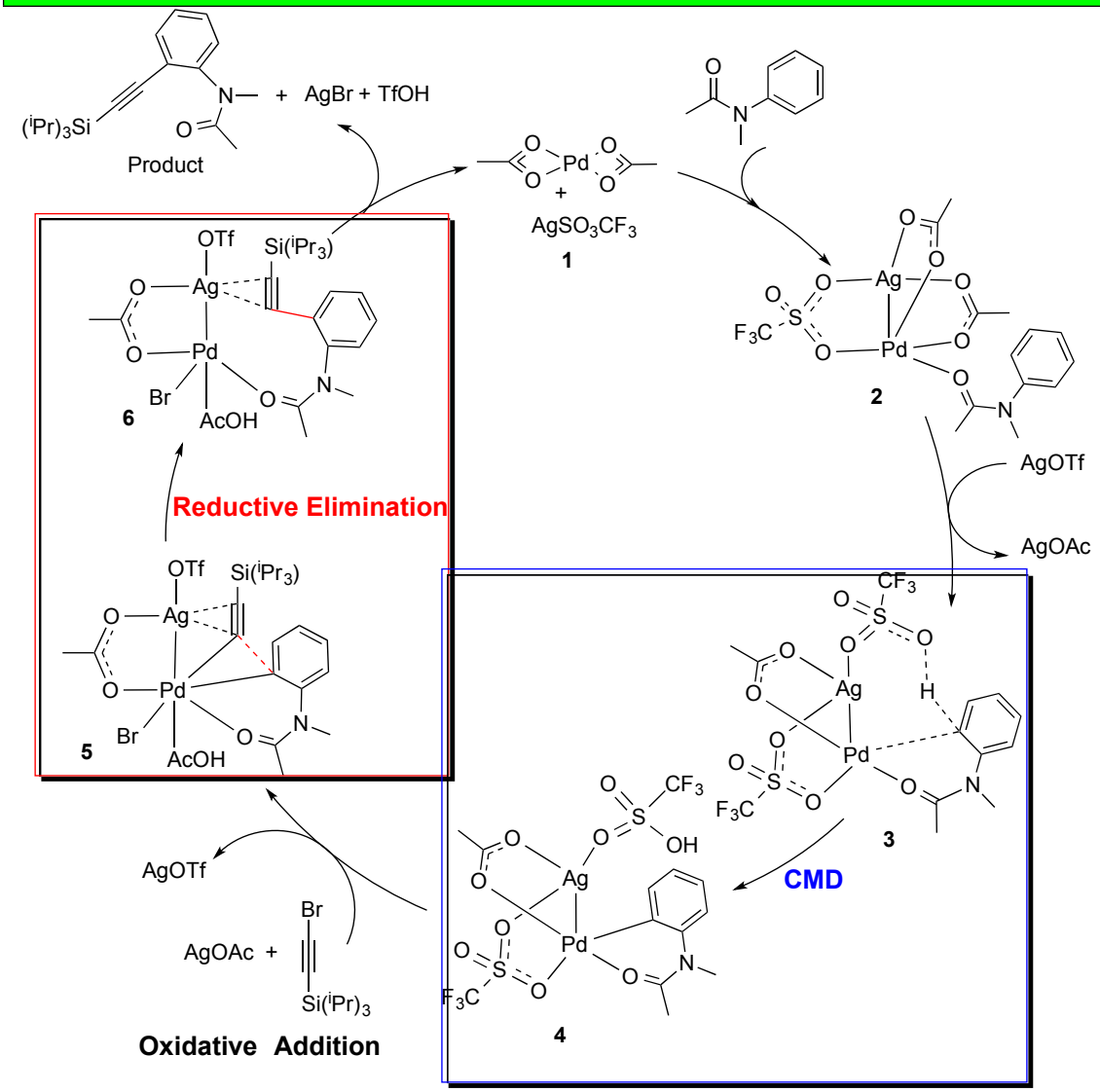
Product
+ AgBr + TfOH
AgSO3CF3
1
2
AgOTf
AgOAc
3
CMD
4
AgOTf
AgOAc +
Oxidative Addition
5
6
Reductive Elimination

Reaction 4

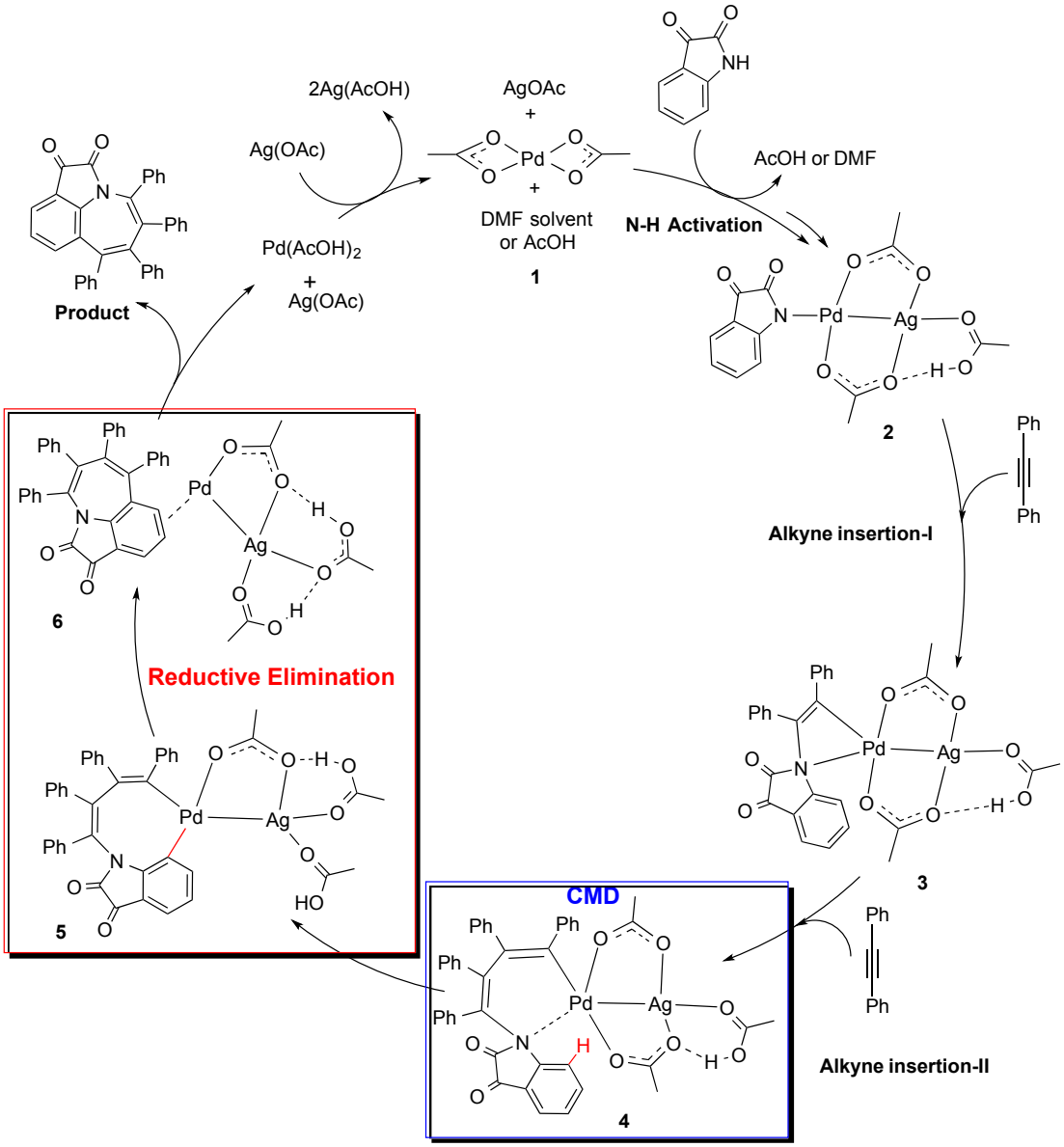
2Ag(AcOH)
AgOAc
+
Ag(OAc)
Pd
+
DMF solvent
or AcOH
1
AcOH or DMF
N-H Activation
Pd(AcOH)2
+
Ag(OAc)
Product
2
Alkyne insertion-I
3
Alkyne insertion-II
CMD
4
Reductive Elimination
5
6

Section 3

Importance of the final products obtained through reactions 1 – 4

Reaction 1

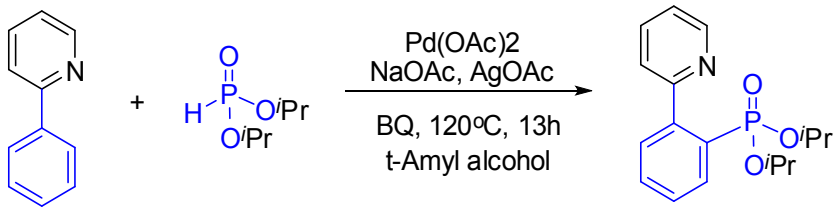

Applications: Aryl phosphonates and derivatives are an important class of molecules because of their broad application in medicinal chemistry.

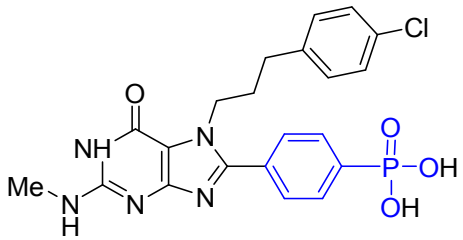

Reaction 2

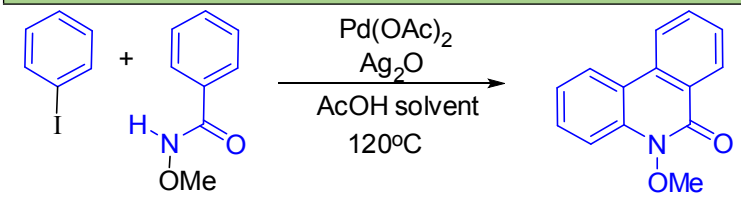

Applications: Quinoline, Quinazoline, and Acridone Alkaloids.[19]

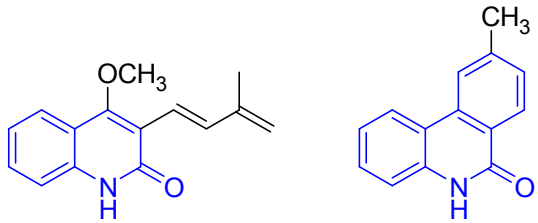

Reaction 3

[19] G. Wurz, O. Hofer and H. Greger, *Nat. Prod. Lett.* 1993, **3**, 177-185.

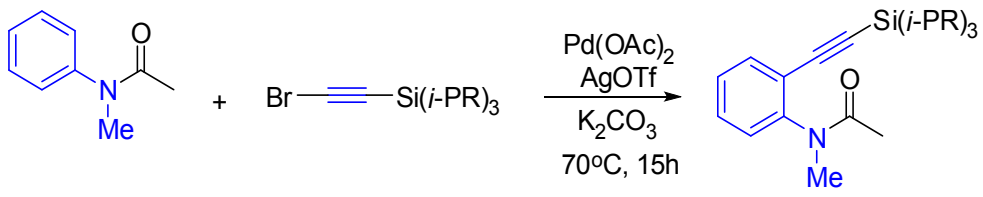

Applications: *Ortho*-alkynylated anilides serve as valuable precursors for indole based heterocycles.[20]

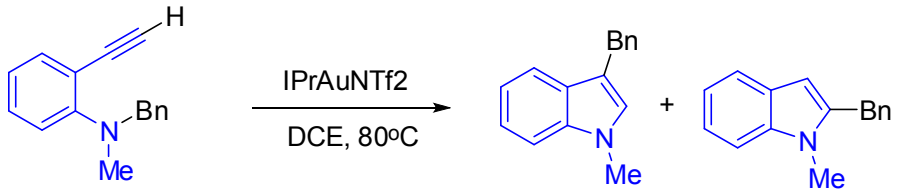

Reaction 4

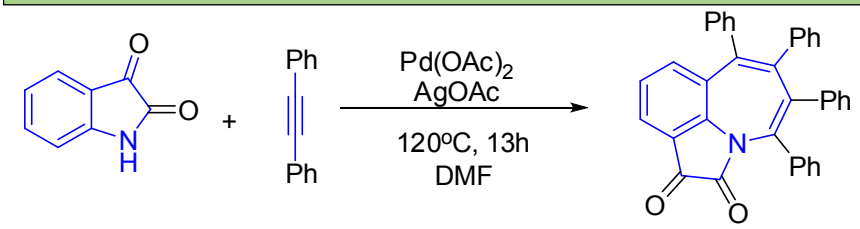

Applications: Benzazepines are well-known seven-membered nitrogen containing heterocycles that form the structural scaffold of many pharmaceutical compounds; therefore, they are often used as structural elements in medicinal chemistry.[21]

(1) **Mozavaptan** is used as an orally effective, nonpeptide arginine vasopressin V-2 receptor antagonist.

(2) **Lotensin** is a prescription medication licensed for treating high blood pressure (hypertension), congestive heart failure, and chronic renal failure by inhibiting angiotensin-converting enzyme (ACE) in human subjects.

---

[20] G. Li, X. Huang and L. Zhang, *Angew. Chem. Int. Ed.* 2008, **47**, 346-349.
[21] L. Wang, J. Huang, S. Peng, H. Liu, X. Jiang, J. Wang, *Angew. Chem. Int. Ed.* 2013, **52**, 1768-1772.

(3) **Anafranil** is identified as an antiobsessional drug that belongs to the class of pharmacologic agents known as tricyclic antidepressants.

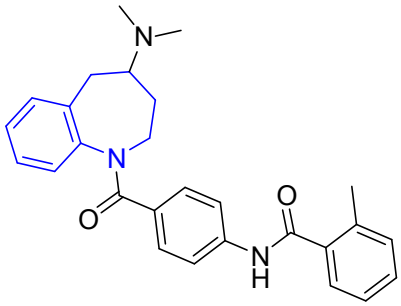

Mozavaptan

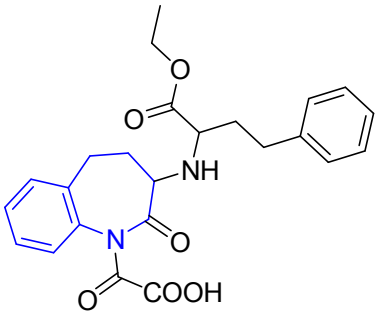

Lotensin

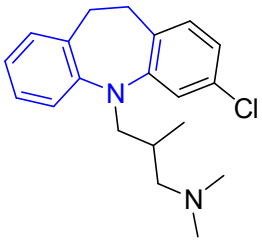

Anafranil

Section 4

Gibbs free energy profiles for reactions 2 – 4

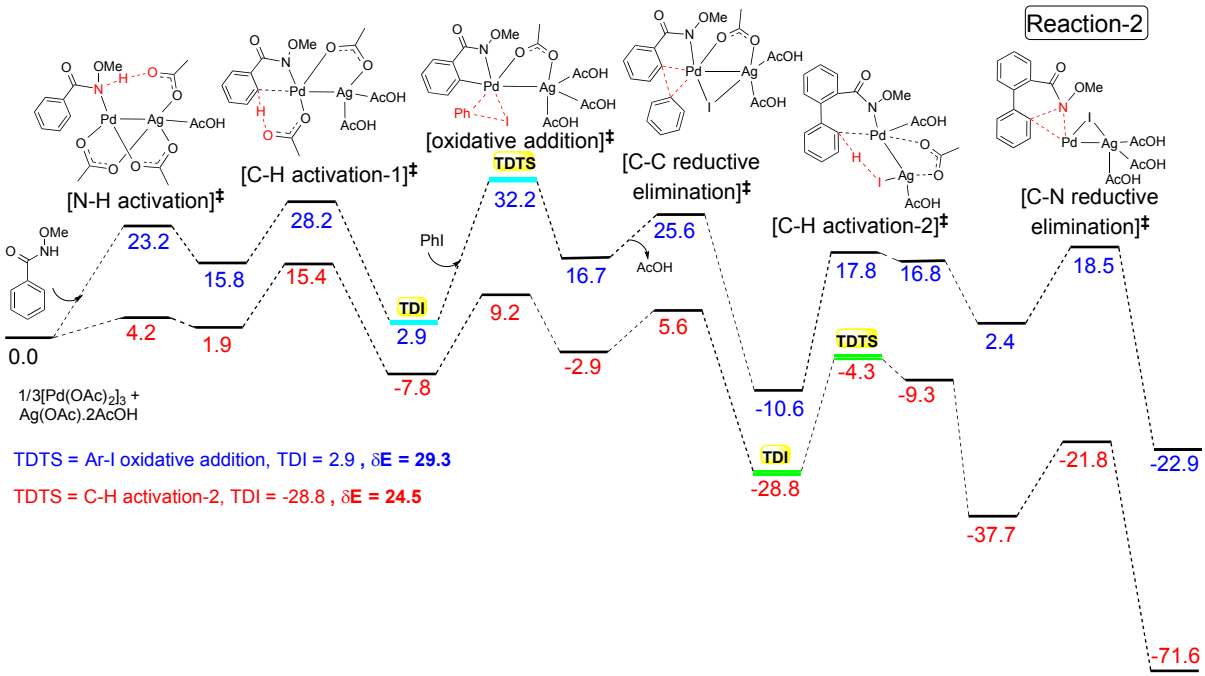

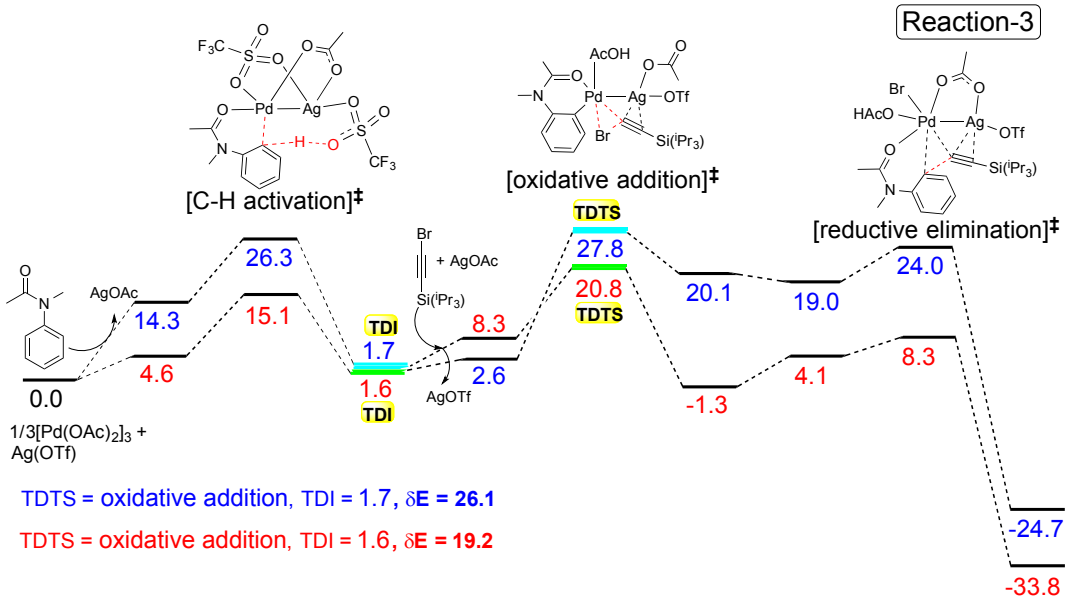

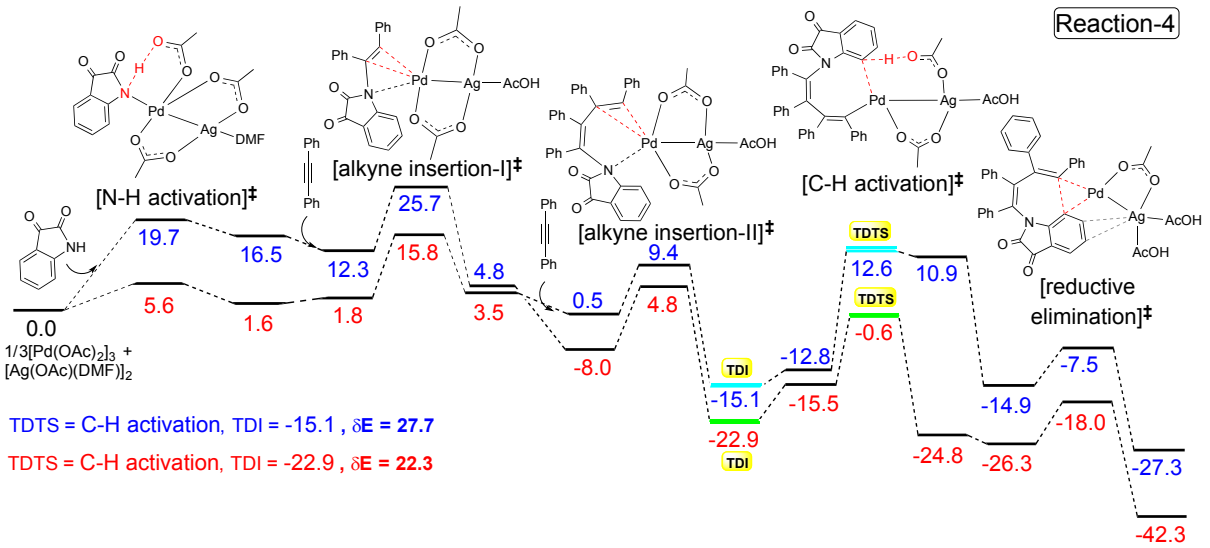

Figure S4. Comparison of the Gibbs free energy profiles for reactions **2** - **4** for the conventional monometallic (blue) and the heterobimetallic Pd-Ag (red) pathways. The calculated energetic span δE and the identity of the turnover determining intermediate (TDI) and turnover determining transition states (TDTS) are shown for each reaction.

A rather surprising stabilization of the reductive elimination TS and intermediates for reaction **2** is noticeable in the heterobimetallic pathway. This can be attributed to a few factors such as (i) the protonation of the bridging acetate by the action of the HI (formed after the second C-H activation) leading to the formation of acetic acid, (ii) formation of an iodo-bridge between Pd and Ag, and (iii) the coordination of three acetic acid molecules on the Ag and their mutual H-bonding. Interesting reports on iodo-bridged Pd complexes are reported, See: (a) Amii, H.; Kageyama, K.; Kishikawa, Y.; Hosokawa, T.; Morioka, R.; Katagiri, T.; Uneyama, K. Preparation, Structure, and Reactions of Trifluoroacetimidoyl Palladium(II) Complexes. *Organometallics* **31**, 1281-1286 (2012). (b) Smith, D. C.; Lake, C. H.; Gray, G. M. Synthesis and characterization of $[Pd_2X_2(\mu\text{-}X)_2\{Ph_2P(CH_2CH_2O)n\text{-}CH_2CH_2PPh_2\text{-}P,P'\}]m$ (n=3, 5, X=Cl, I) dimetallacrown ethers and the related dinuclear $[Pd_2Cl_2(\mu\text{-}Cl)_2\{Ph_2P(CH_2)_{12}PPh_2\text{-}P,P'\}]m$ and

[$Pd_2X_2(\mu\text{-}X_2)\{Ph_2P(CH_2CH_2O)_2CH_2CH_3\text{-}P)_2\}$] (X=Cl, I) complexes. *Dalton Trans*. **2003**, 2950-2955. (c) Ding, Y.; Goddard, R.; Porschke, K. R. Cationic Dinuclear Pd-Allyl-Halide Complexes with N-Heterocyclic Carbenes. *Organometallics* **2005**, *24,* 439-445.

The computed ΔG for breaking of Ag_2O into AgOAc (i.e., $Ag_2O + 2AcOH \rightarrow 2AgOAc + H_2O$) is found to be -72.6 kcal/mol at the SMD_{AcOH}/M06/6-31G**,LANL2TZ(f)(Ag)//SMD_{AcOH}/M06/6-31G**,LANL2DZ(Ag) level of theory. The conversion of Ag_2O is therefore favorable, facilitating its participation in the formation of Pd-Ag heterobimetallic species. See the following references for the formation of AgOAc from Ag_2O.

(a) Lebrasseur, N.; Larrosa, I. *J. Am. Chem. Soc*. **2008**, *130*, 2926-2927. (b) Chun, S.; Grudinin, D.; Lee, D.; Kim, S.-H.; Yi, S.-G.; Hwang, I. *Chem. Mater.* **2009,** *21,* 343–350. (c) Wang, H.; Wan, C.-Q.; Yang, J.; Mak, T. C. W. *Cryst. Growth Des*. **2014**, *14*, 3530−3540. (d) Hayes, J. M.; Viciano, M.; Peris, E.; Gregori Ujaque, G.; Lledos, A. *Organomet.* **2007,** *26,* 6170-6183.

Section 5

Optimized geometries of CMD and RE transition states in the condensed phase

Note on nomenclature for different stationary points (intermediates and transition states) used in this document is as follows, The first number refers to the reaction, subscripts CH and RE respectively stands for 'C-H activation' and 'Reductive Elimination' steps of a given reaction. Additional numerical subscript immediately following CH or RE refers to the position of the transition states identified from a larger set of such possibilities (e.g., see Section 5).

Note: The relative Gibbs free energies of the transition states are obtained at the $SMD_{(solvent)}$/M06/6 31G(d,p)/LANL2TZ(f)(Pd,Ag), LANL2DZ(d,p)(Br, I) level of theory using the geometries (and thermal and entropic corrections) from the $SMD_{(solvent)}$/M06/6-31G**,LANL2DZ level of theory. The values in parentheses are obtained at the $SMD_{(solvent)}$/M06/6 31G**,LANL2DZ(Pd,Ag,Br,I) level of theory.

Pd | Pd-Ag

CMD

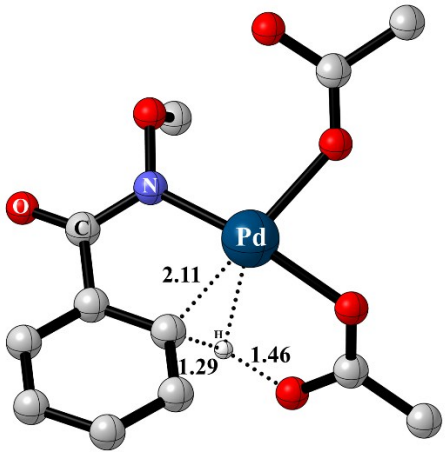

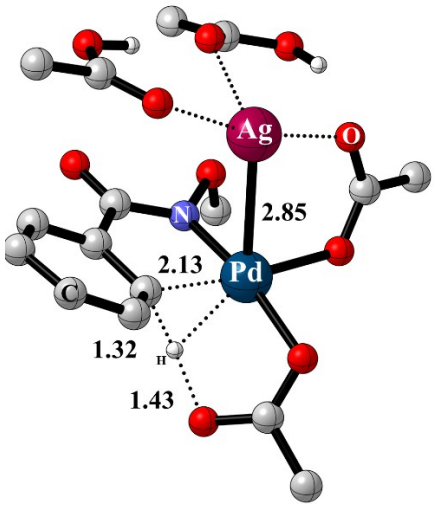

2$_{\mathbf{CH1(Pd)}}$

ΔG = 28.1 (27.3)

2$_{\mathbf{CH1(Pd–Ag)}}$

ΔG = 15.4 (14.5)

RE

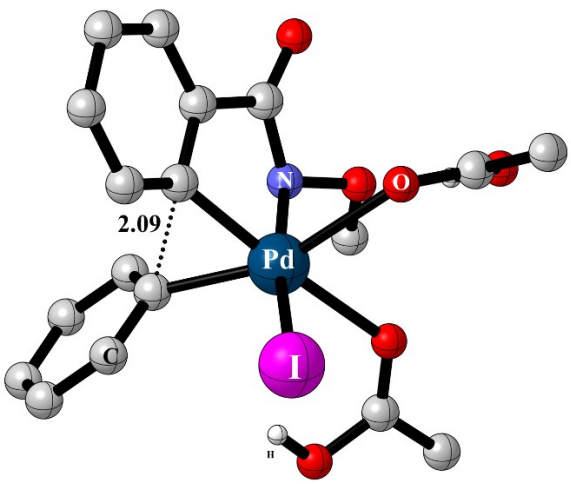

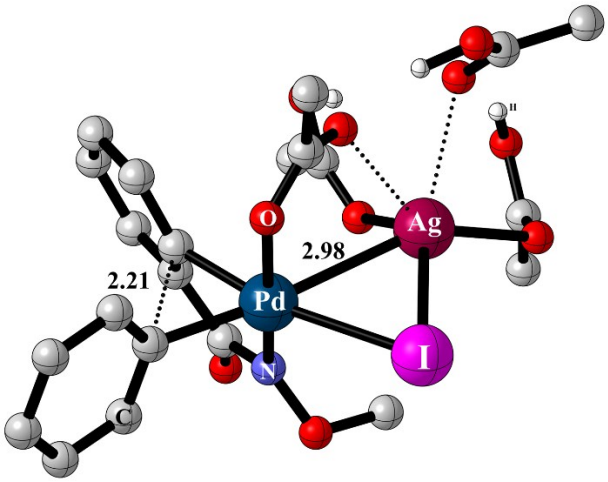

2$_{\mathbf{RE1(Pd)}}$

ΔG = 25.5 (22.5)

2$_{\mathbf{RE1(Pd–Ag)}}$

ΔG = 6.3 (4.3)

Figure S5.1: Reaction-**2**

Pd

Pd-Ag

CMD

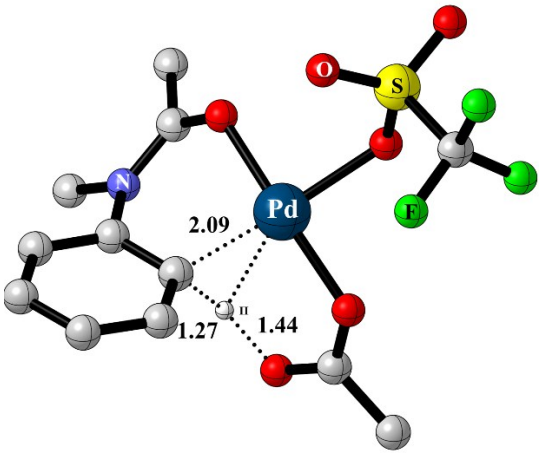

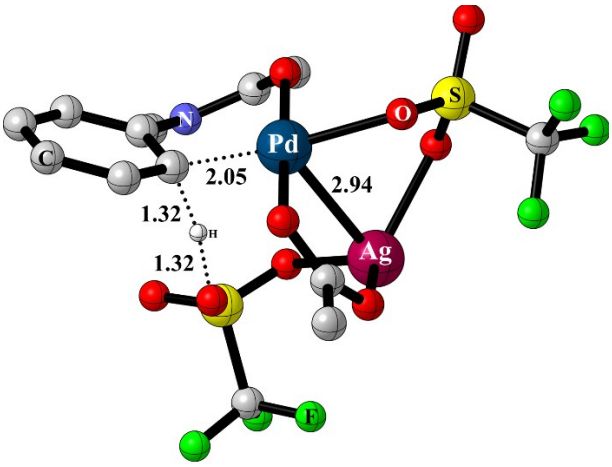

3$_{\mathbf{CH1(Pd)}}$

ΔG = 26.2 (26.1)

3$_{\mathbf{CH1(Pd—Ag)}}$

ΔG = 15.0 (14.6)

RE

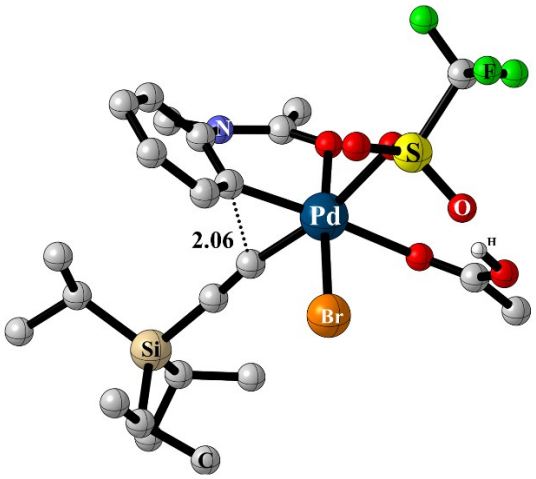

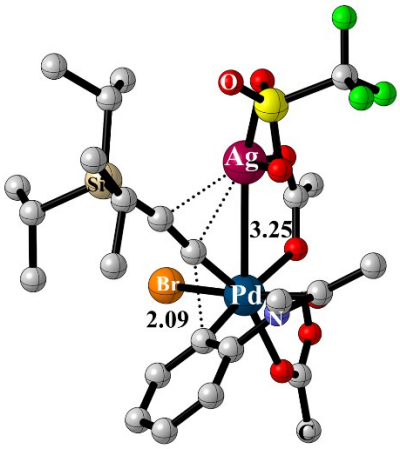

3$_{\mathbf{RE1(Pd)}}$

ΔG = 23.8 (18.7)

3$_{\mathbf{RE1(Pd—Ag)}}$

ΔG = 8.2 (3.0)

Figure S5.2: Reaction-**3**

Pd

Pd-Ag

CMD

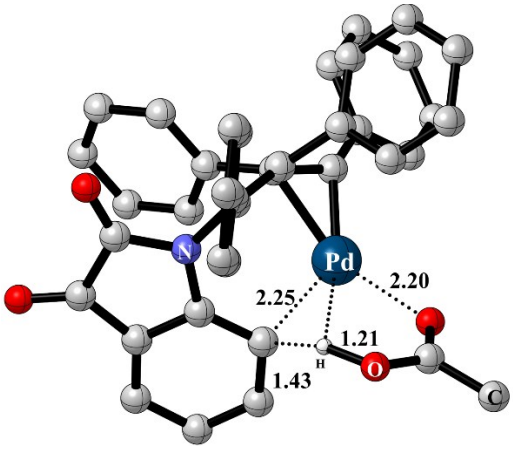

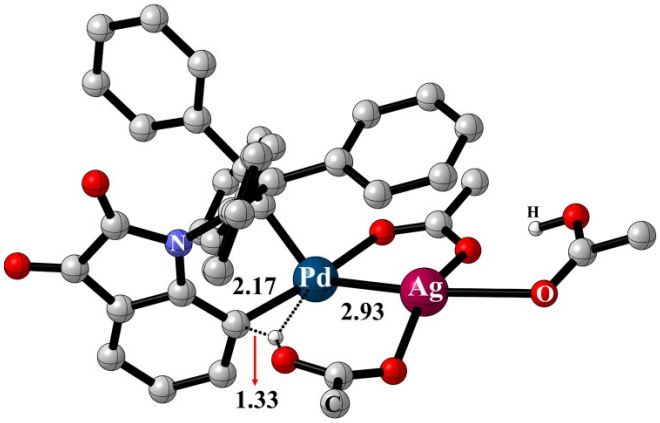

4$_{\mathbf{CH1(Pd)}}$

ΔG = 14.3 (10.4)

4$_{\mathbf{CH1(Pd—Ag)}}$

ΔG = 4.3 (-1.2)

RE

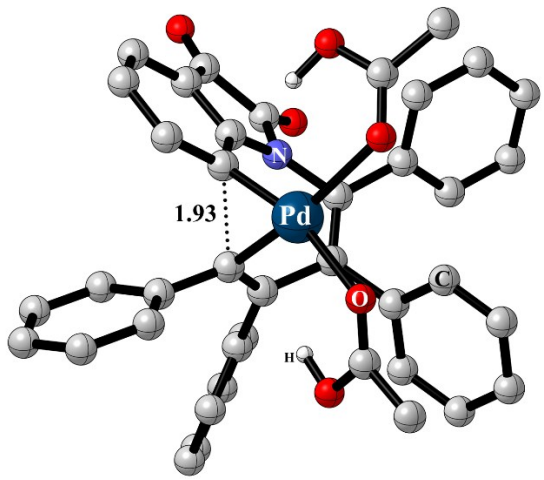

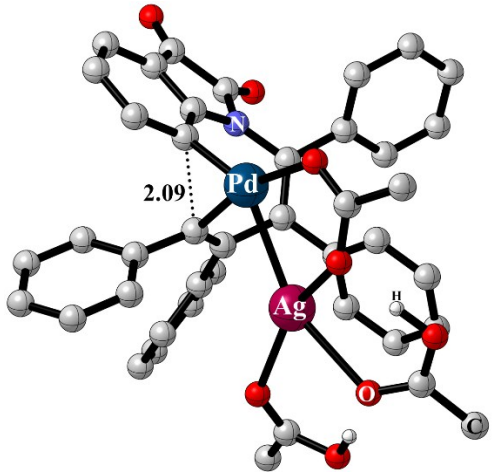

$\mathbf{4}_{\mathbf{RE1(Pd)}}$

ΔG = -5.9 (-11.3)

$\mathbf{4}_{\mathbf{RE1(Pd—Ag)}}$

ΔG = -16.1 (-19.0)

Figure S5.3: Reaction-**4**

Section 6
Stacking of Transition States

Section 6.1: Stacking of Transition States for Reactions **1** to **4**. Stacking of transition states generated through conformational and configurational sampling and the corresponding relative free energies with respect to the lowest energy transition state obtained at the $SMD_{(solvent)/}$M06/6-31G**/LANL2DZ(Pd,Ag,Br,I) level of theory. Shown in the rectangular insets are the most preferred ones for the monometallic (in red color) and heterobimetallic (blue color) transition states. The nomenclature used is as follows. The C-H activation transition states via a cyclometallation deprotonation (CMD) are given a generic representation using subscript "$_{CH}$". The numerical prefix pertains to the reaction. The numerical suffix is assigned on the basis of the position of a given transition state with respect to the lowest energy transition state. The monometallic and heterobimetallic transition states are respectively designated by using "Pd" or "Pd-Ag" in parentheses. Similar notations are followed for the reductive elimination (denoted as "$_{RE}$" instead) as well.

Reaction 1

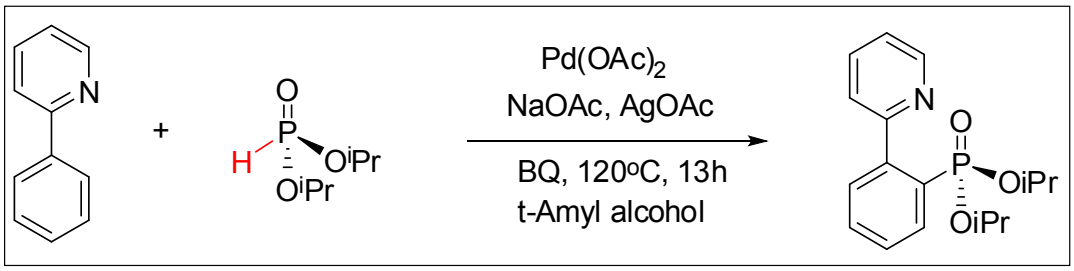

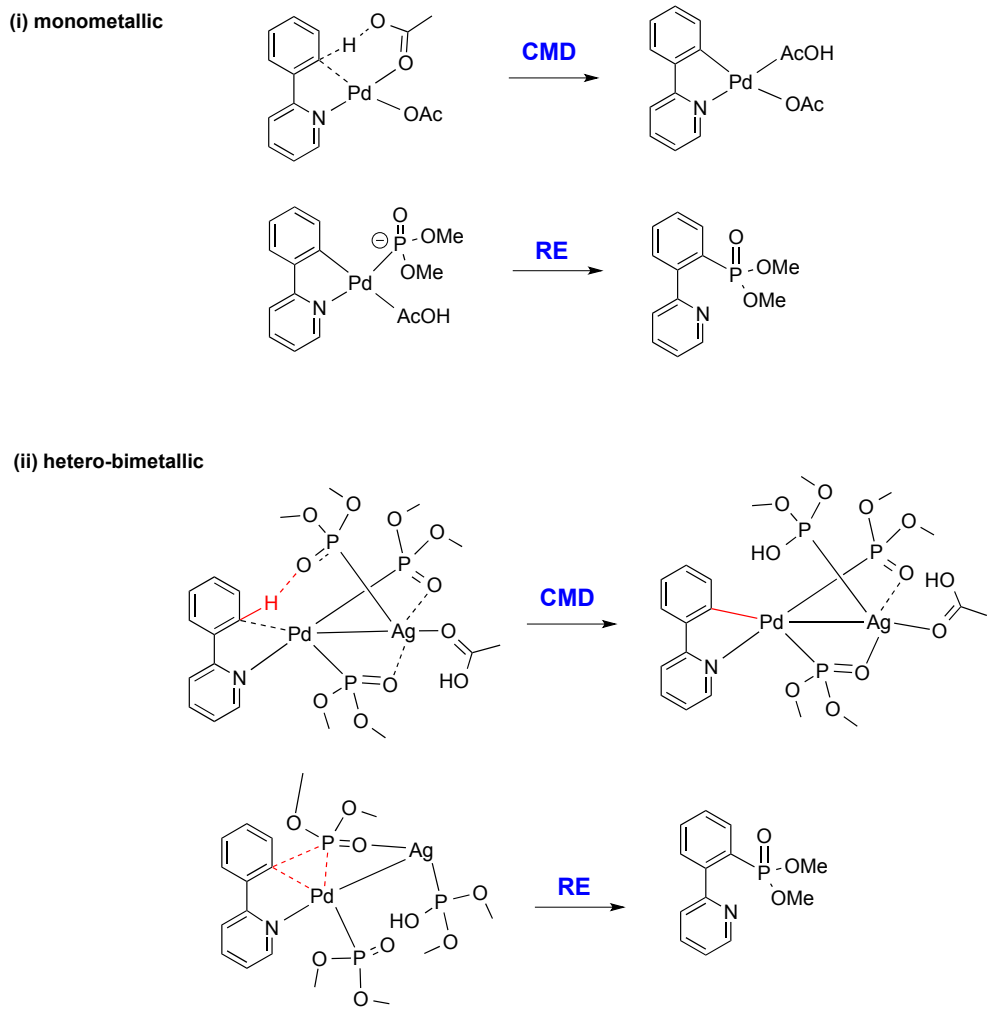

Figure S6.1: Reaction conditions and important transition states for reaction **1**.

Reaction 1

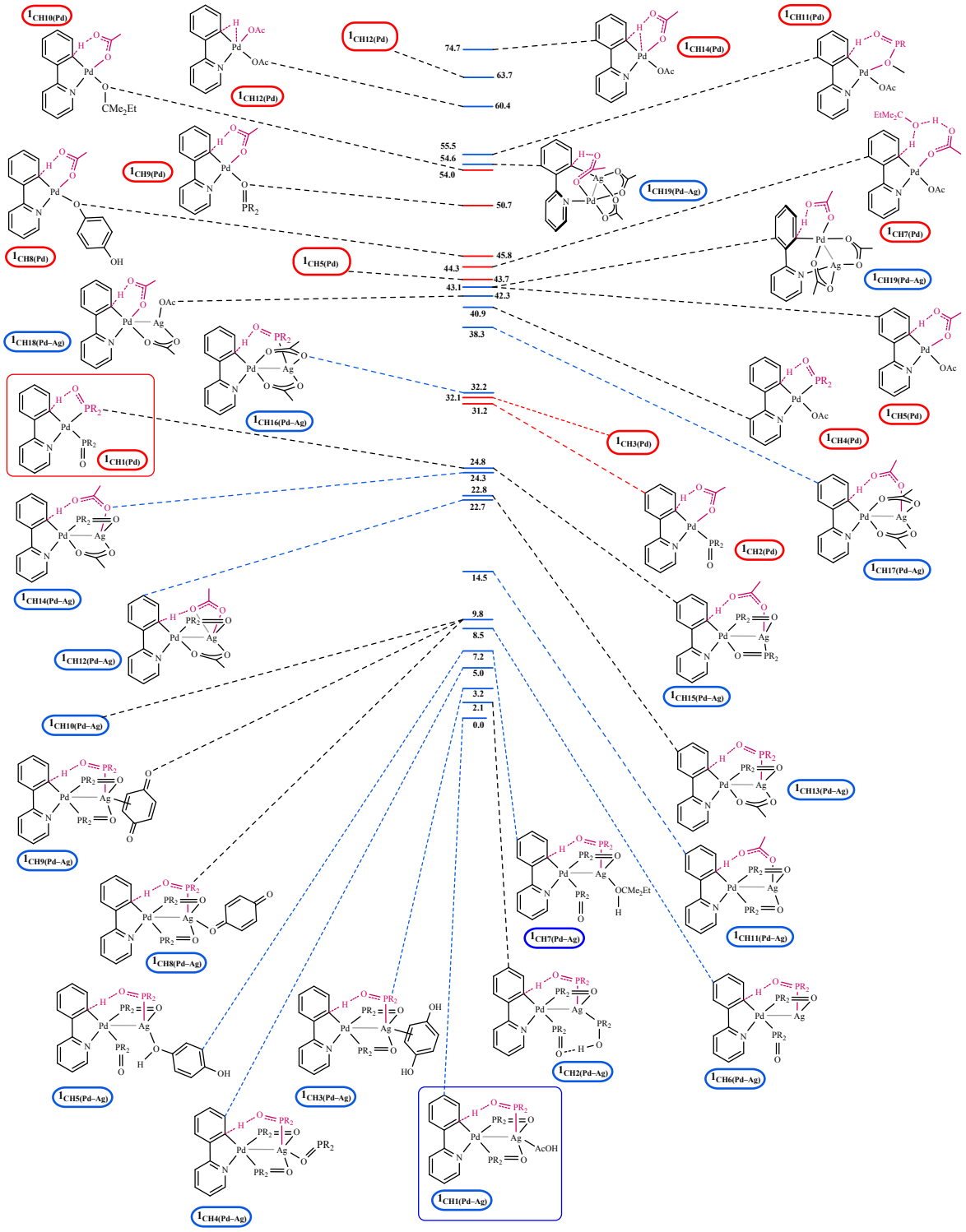

Figure S6.2: Stacking of CMD transition states.

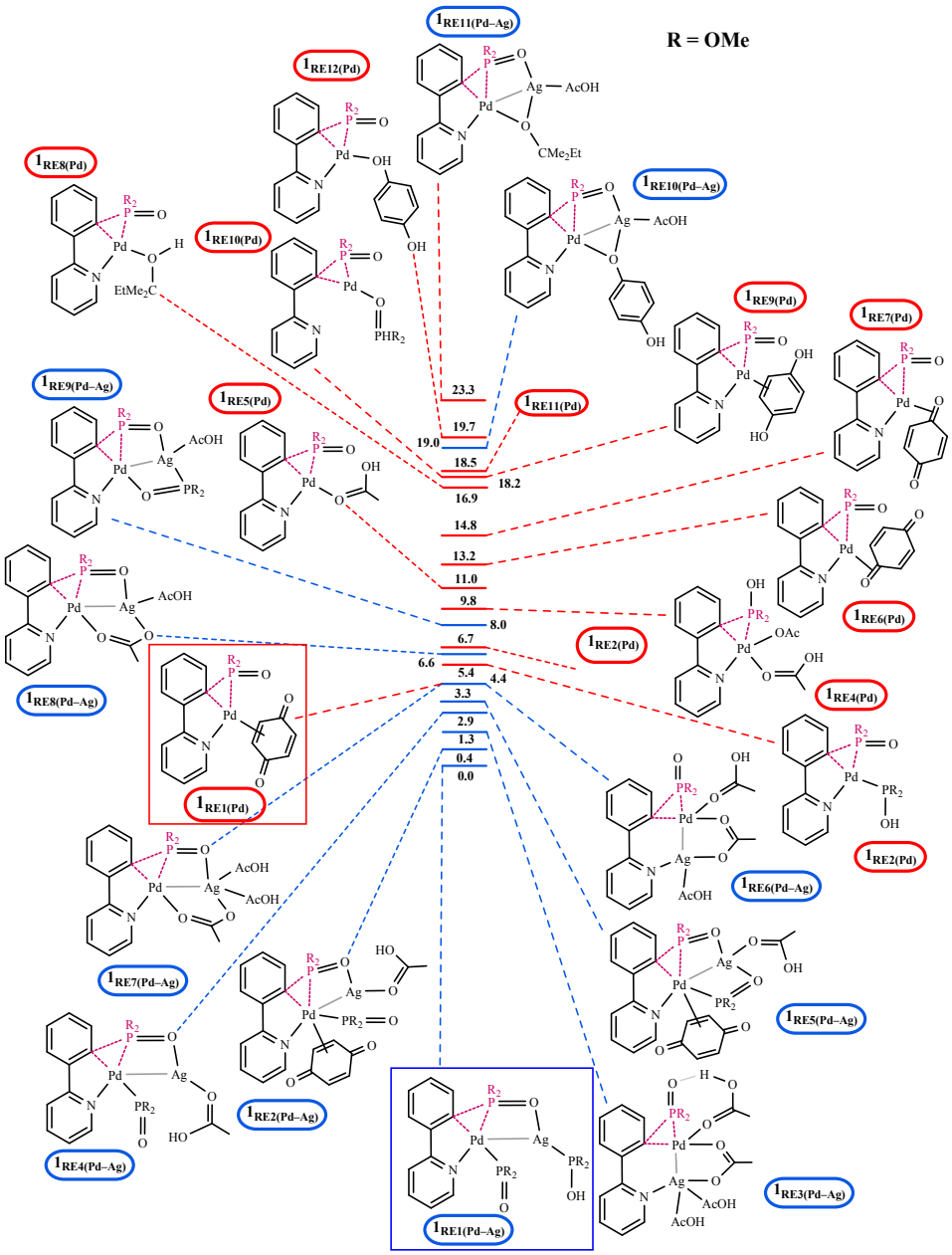

Figure S6.3: Stacking of RE transition states

Reaction 2

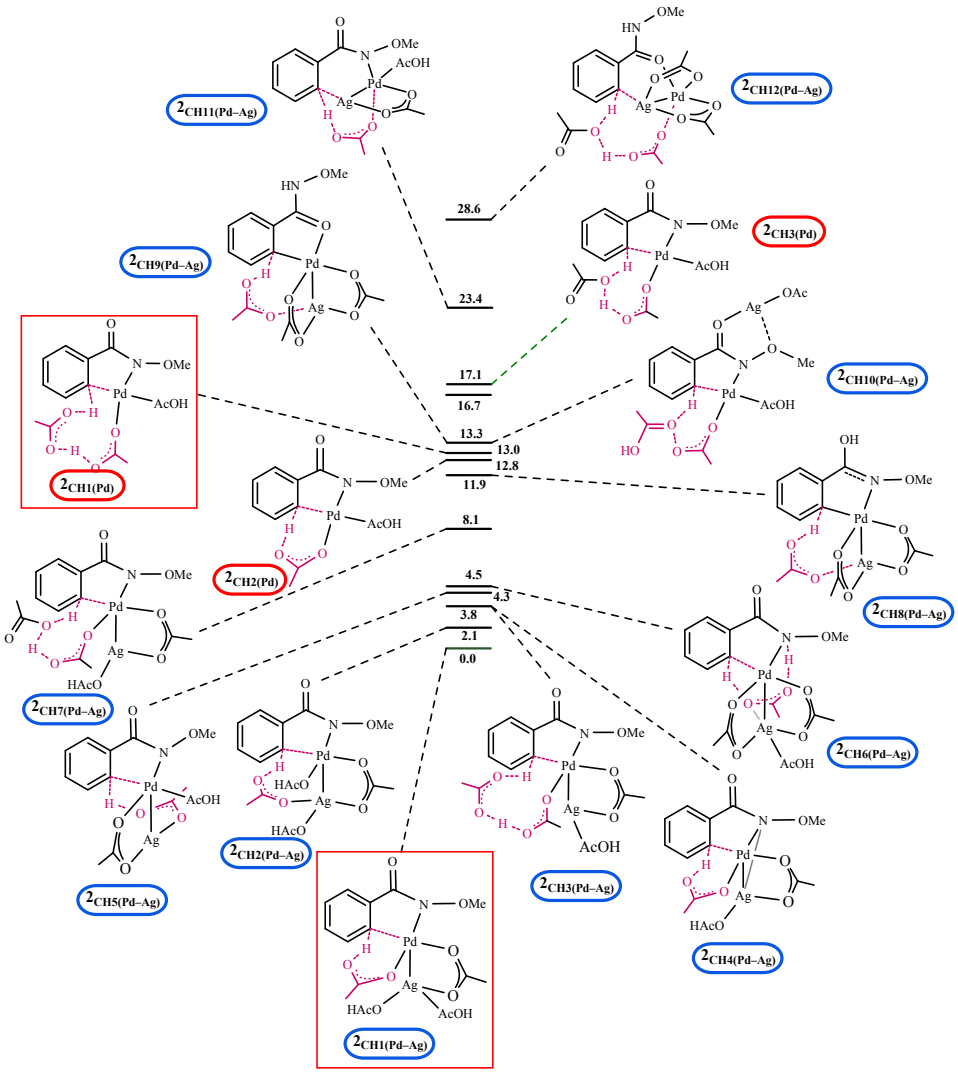

Figure S6.4: Stacking of CMD transition states.

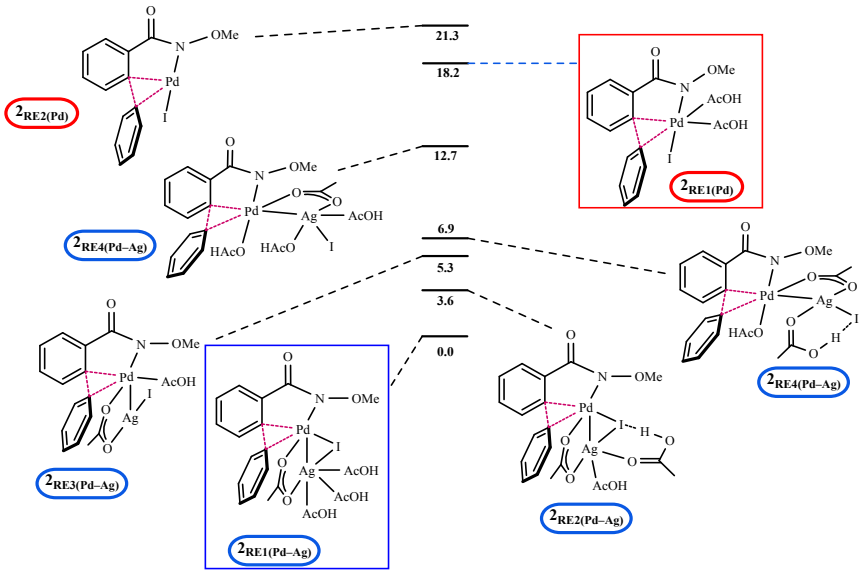

Figure S6.5: Stacking of RE transition states.

Reaction 3

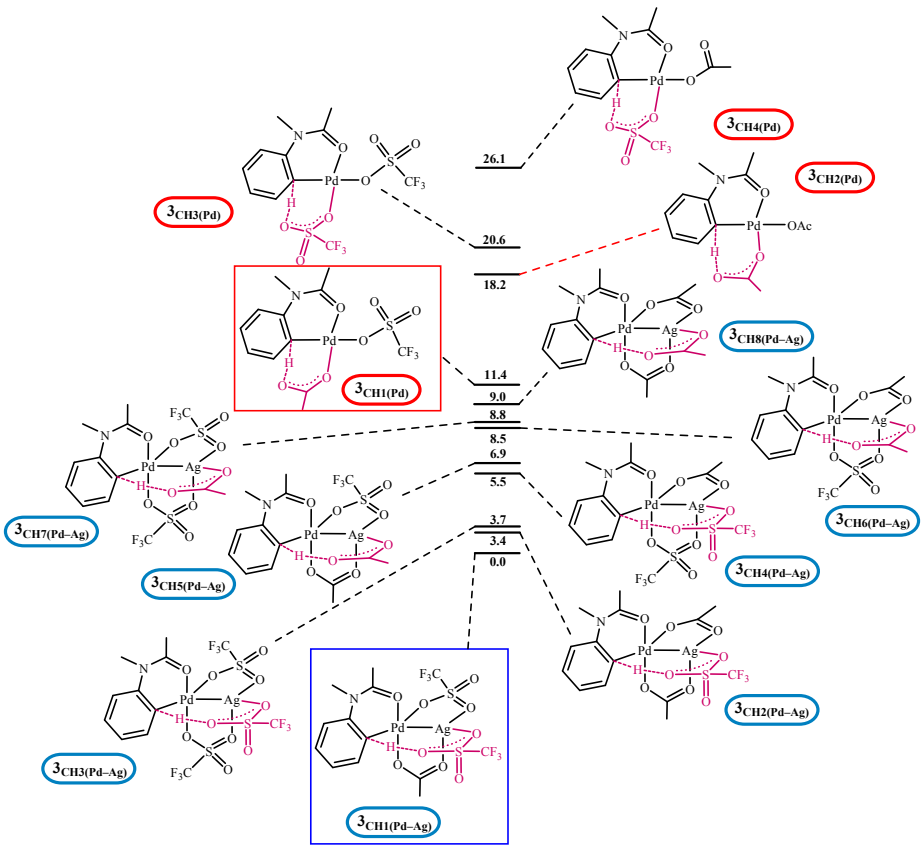

Figure S6.6: Stacking of CMD transition states.

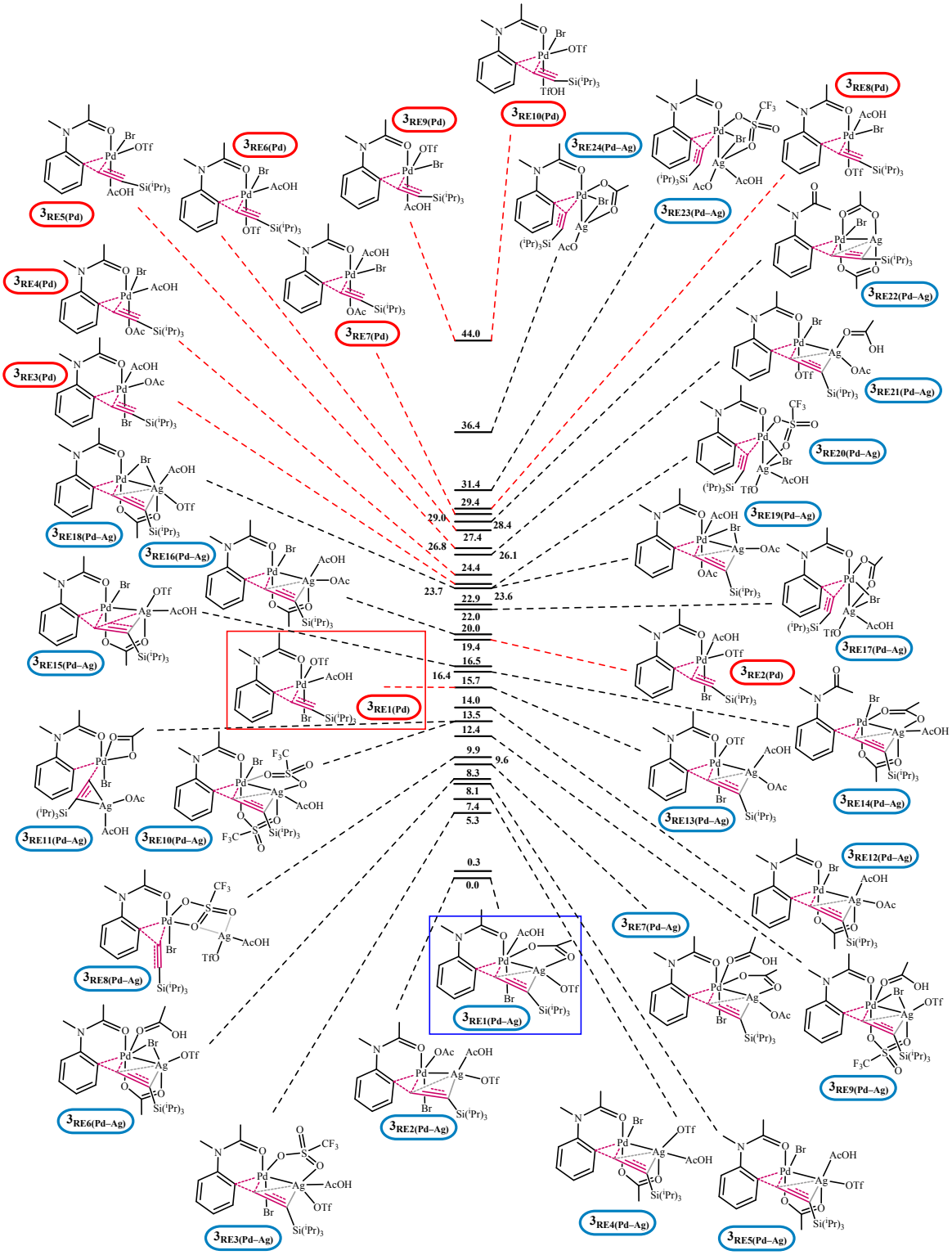

Figure S6.7: Stacking of RE transition states.

Reaction 4

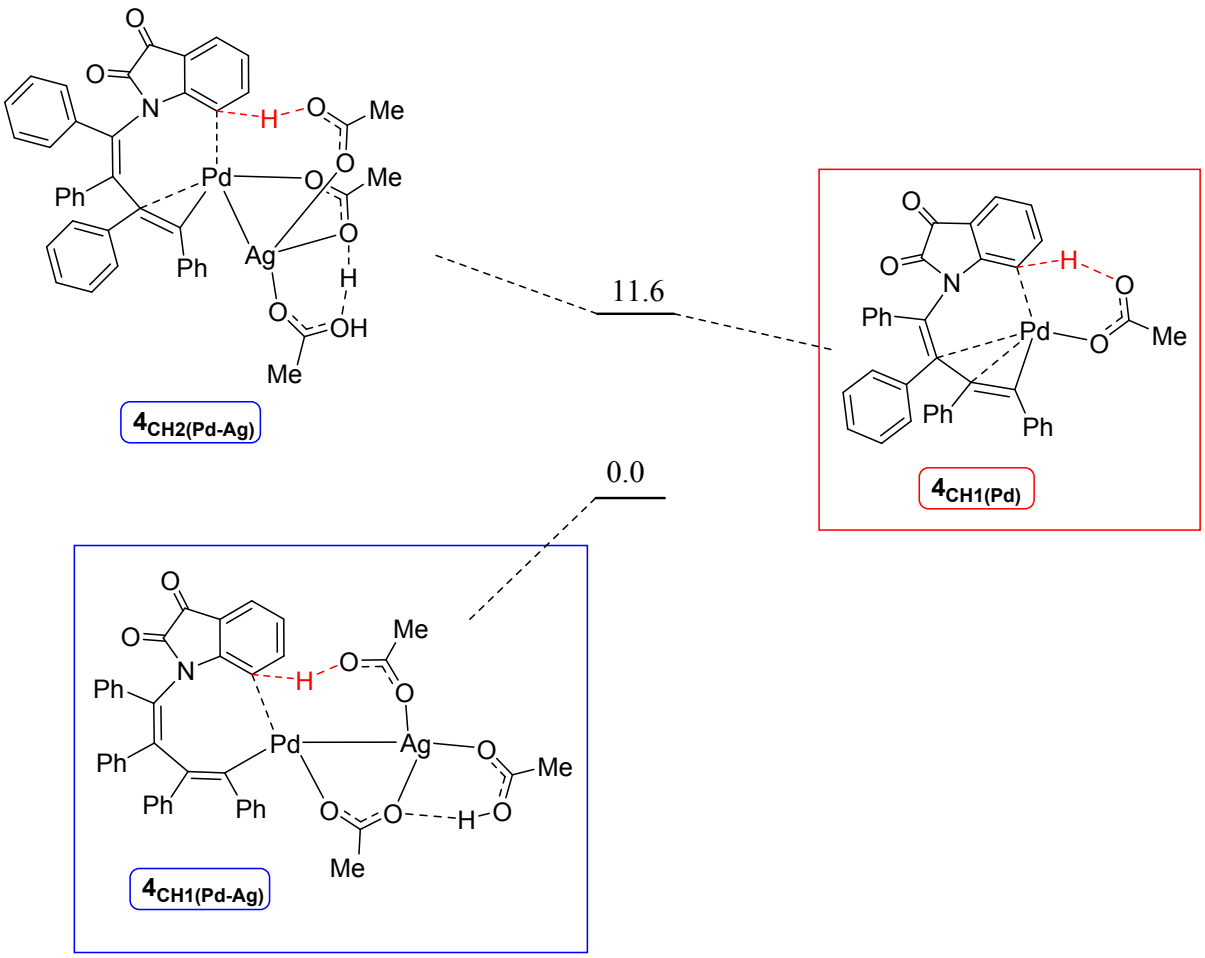

Figure S6.8: Stacking of CMD transition states.

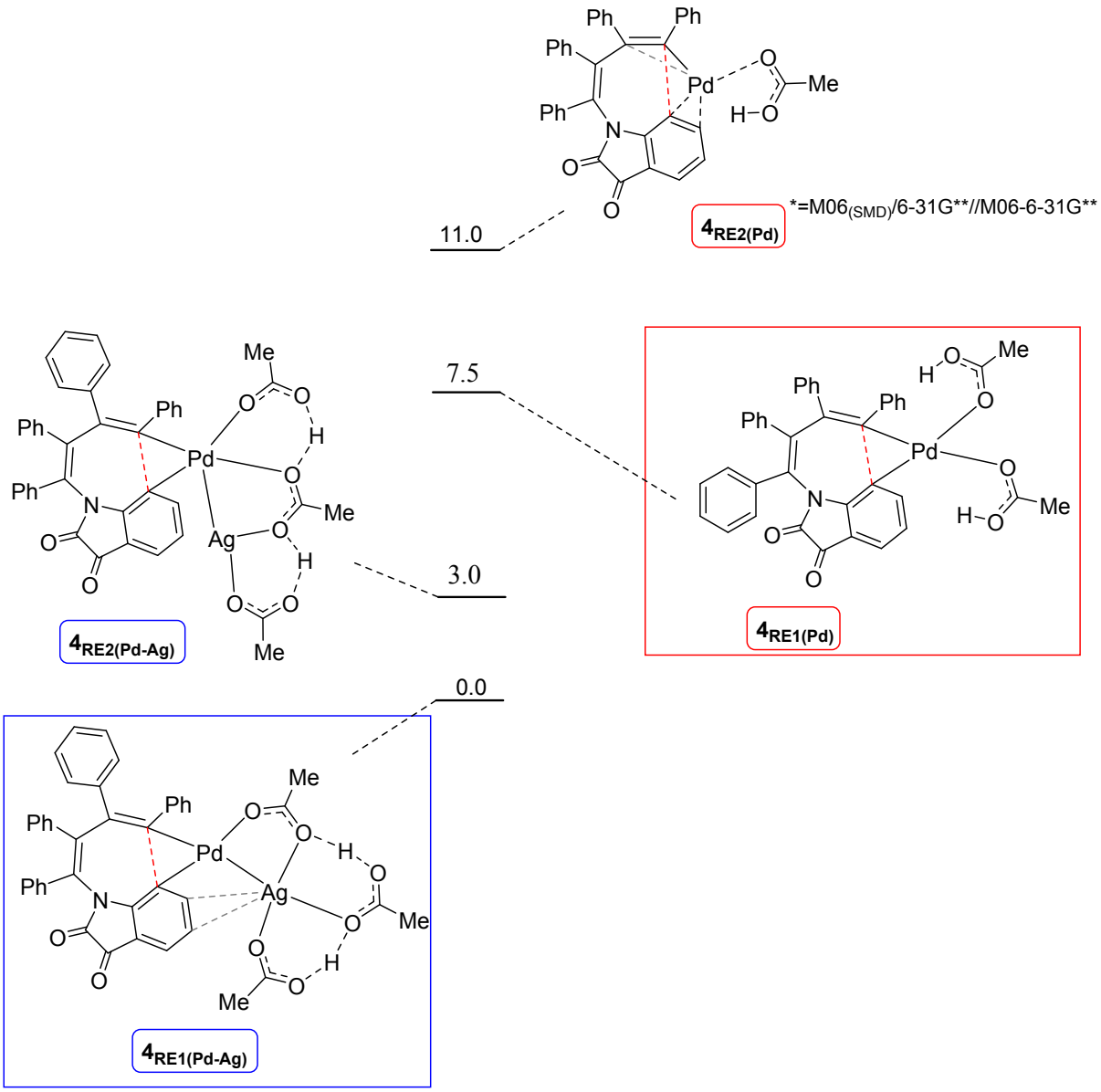

Figure S6.9: Stacking of RE transition states.

Section 7

General Geometric Features of the Transition States

7.1: C–H activation via Cyclometallation Deprotonation (CMD)

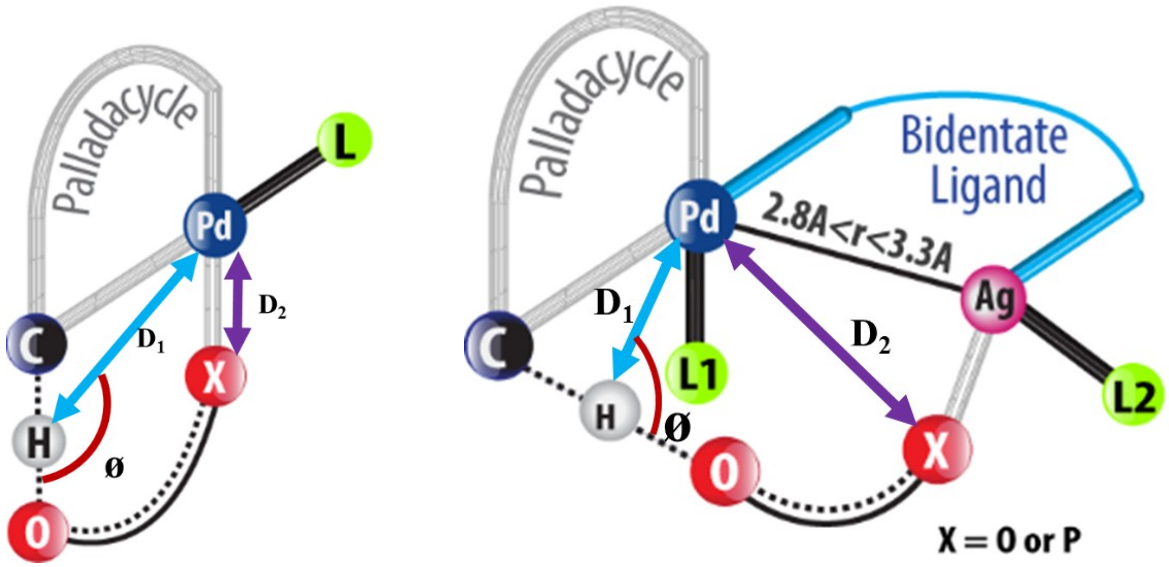

Figure S7.1. Geometric parameters for the C–H activation transition state leading to cyclometallation. $\mathbf{D_1}$ and $\mathbf{D_2}$ are in Å. **Ø** is the bond angle between Pd–H–O.

Table S7.1: Important Structural Parameters of the Cyclometalliation Deprotonation Transition States

Reaction	D_1	D_2	Ø
$\mathbf{1}_{CH1(Pd)}$	2.28	2.26	105.3
$\mathbf{1}_{CH1(Pd–Ag)}$	2.31	3.65	125.0
$\mathbf{2}_{CH1(Pd)}$	2.00	2.90	112.5
$\mathbf{2}_{CH1(Pd–Ag)}$	1.97	2.86	113.2
$\mathbf{3}_{CH1(Pd)}$	2.07	2.04	109.0
$\mathbf{3}_{CH1(Pd–Ag)}$	2.19	3.88	127.0
$\mathbf{4}_{CH1(Pd)}$	2.27	2.19	116.7
$\mathbf{4}_{CH1(Pd–Ag)}$	2.47	4.04	148.8

In general, the Pd–H distance (**D_1**) is slightly longer and Pd-H-O bond angle (**ø**) is wider in the case of Pd–Ag. This geometric feature can be regarded as lowering the strain in the CMD transition state due to the involvement of silver in the TS, as shown above through a generalized representation. A closer inspection of reaction **2** reveals that ligand involved in CMD (**X**) remains attached to Pd (for all the other cases it is bound to Ag), making it very similar to the TS without any Ag. This suggests that some communication, in addition to the 'geometric relaxation' provided by Pd–Ag interaction, may also help stabilize the TSs. Hence, we have analyzed the orbital interactions responsible for the stabilization of the transition states.

7.2: Reductive Elimination

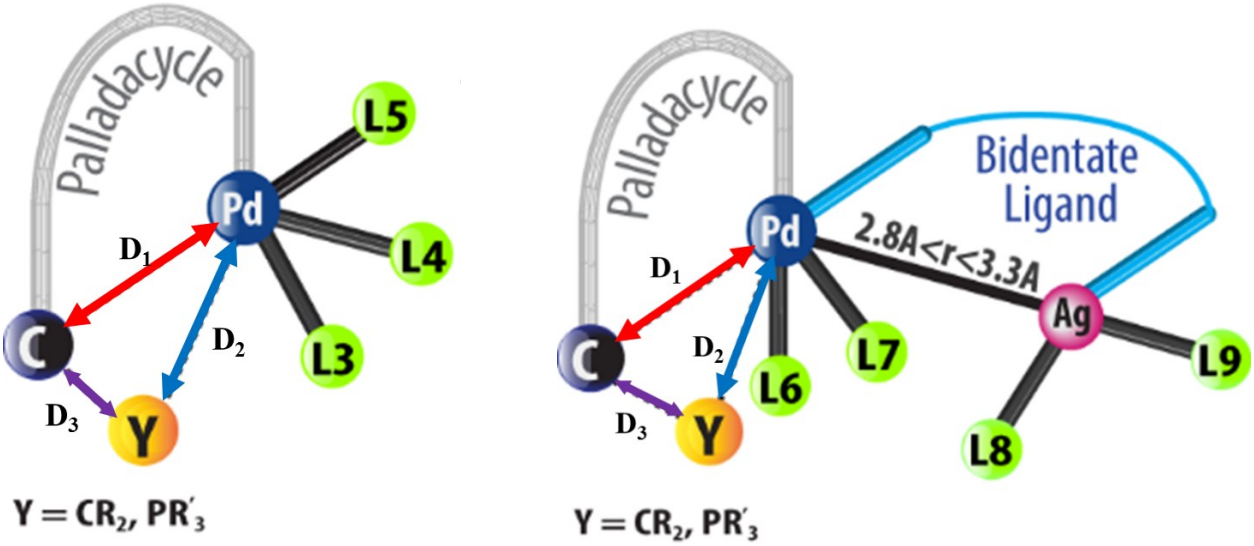

Figure S7.2. Geometric parameters for the reductive elimination (RE) transition state. **D_1**, **D_2** and **D_3** are in Å. **$Ø_1$**, **$Ø_2$** and **$Ø_3$** are angles between **D_1-D_2**, **D_2-D_3** and **D_3-D_1** respectively.

Table S7.2: Important Structural Parameters of the Reductive Elimination Transition States

Reaction	D_1	D_2	D_3	$Ø_1$	$Ø_2$	$Ø_3$
$1_{RE1(Pd)}$	2.09	2.32	2.44	66.9	51.9	61.2
$1_{RE1(Pd–Ag)}$	2.11	2.32	2.26	61.0	54.9	64.0
$2_{RE1(Pd)}$	2.06	2.13	2.09	59.9	58.5	61.6
$2_{RE1(Pd–Ag)}$	2.06	2.10	2.22	64.3	56.9	58.8

$3_{RE1(Pd)}$	2.06	1.95	2.06	61.8	61.7	56.5
$3_{RE1(Pd–Ag)}$	2.10	1.97	2.09	62.5	60.8	56.7
$4_{RE1(Pd)}$	2.06	2.06	1.93	55.9	62.4	61.7
$4_{RE1(Pd–Ag)}$	2.05	2.03	2.10	61.8	59.6	58.7

Section 8
Natural Bond Orbitals Analysis

8.1: (A) Population of d-orbitals on palladium

Table S8.1: Details of d-orbital population and NPA charge on the Pd center, as given by natural population analysis, for various transition states for reactions **1** – **4** obtained at the $SMD_{(solvent)}$/M06/6-31G**,LANL2DZ(Pd,Ag,Br,I) level of theory. The relative occupancy refers to the occupancy in the Pd-Ag heterobimetallic TS as compared to that in the monometallic Pd TS

TS	d-orbital occupancy on Pd	relative occupancy	charge on Pd	relative charge on Pd	charge on Ag
$\mathbf{1}_{CH1(Pd)}$	9.295	0.000	-0.236	0.000	-
$\mathbf{1}_{CH1(Pd—Ag)}$	9.283	-0.012	-0.194	+0.042	0.395
$\mathbf{1}_{RE1(Pd)}$	9.192	0.000	0.166	0.000	-
$\mathbf{1}_{RE1(Pd—Ag)}$	9.382	+0.19	-0.216	-0.382	0.400
$\mathbf{2}_{CH1(Pd)}$	8.931	0.000	0.543	0.000	-
$\mathbf{2}_{CH1(Pd—Ag)}$	8.925	-0.006	0.439	-0.105	0.759
$\mathbf{2}_{RE1(Pd)}$	8.913	0.000	0.280	0.000	-
$\mathbf{2}_{RE1(Pd—Ag)}$	8.870	-0.043	0.303	+0.023	0.545
$\mathbf{3}_{CH1(Pd)}$	8.881	0.000	0.613	0.000	-
$\mathbf{3}_{CH1(Pd—Ag)}$	8.892	+0.011	0.519	-0.094	0.739
$\mathbf{3}_{OA(Pd)}$	8.881	0.000	0.344	0.000	-
$\mathbf{3}_{OA(Pd—Ag)}$	8.882	+0.001	0.449	+0.105	0.129
$\mathbf{3}_{RE1(Pd)}$	8.783	0.000	0.383	0.000	-
$\mathbf{3}_{RE1(Pd—Ag)}$	8.767	-0.016	0.359	-0.024	0.719

$4_{CH1(Pd)}$	9.122	0.000	0.343	0.000	-
$4_{CH1(Pd—Ag)}$	9.124	+0.002	0.426	+0.079	0.698
$4_{RE1(Pd)}$	9.313	0.000	0.220	0.000	-
$4_{RE1(Pd—Ag)}$	9.261	-0.052	0.143	-0.077	0.692

8.2: (B) Details of selected set of donor-acceptor interactions between the metals and ligands

Note-1: Numbering is shown only for the important atoms that are involved in key delocalizations

Note-2: For easier identification, the important donor-acceptor interactions between the natural atomic orbitals are highlighted in the following tables. The selection of the donor-acceptor interactions are based on (a) sufficiently large second-order perturbation energies, and (b) the participation of d-orbitals on palladium. These natural atomic orbitals (NAO) (e.g., p_x, p_y, p_z, d_{x2-y2}, d_{z2}, d_{xy}, d_{yz}, d_{xz}) as well as natural bond orbitals (NBO) (e.g., $\sigma_{X–Y}$, $\sigma^*_{X–Y}$, $\pi_{C=Z}$, $\pi^*_{C=Z}$) are identified on the basis of the relative coefficients as noted in the NBO3.0 program output. In situations where the NAOs were not quite explicitly clear, we have assigned the nature of NAO on the basis of the highest coefficient.

Reaction 1

Table S8.2: Electron Occupancies in Palladium d-orbitals in the CMD Transition States

TS	orbitals involved	occupancy	relative occupancy	overall occupancy
$1_{CH1(Pd)}$	d(xy)	1.476	0.000	9.295
	d(yz)	1.969		
	d(xz)	1.937		
	d(x^2-y^2)	1.954		

	d(z^2)	1.960		
$1_{CH1(Pd—Ag)}$	d(xy)	1.898	+0.422	9.283
	d(yz)	1.919	-0.050	
	d(xz)	1.652	-0.285	
	d(x^2-y^2)	1.956	+0.001	
	d(z^2)	1.859	-0.101	

CMD

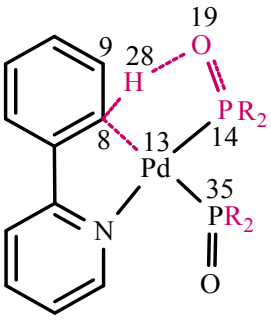

$1_{CH1(Pd)}$

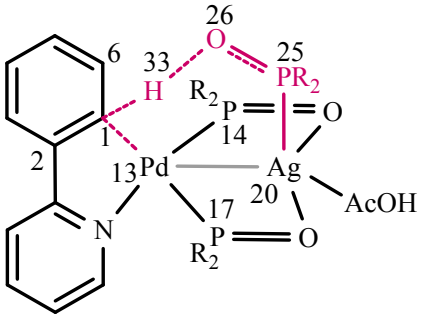

$1_{CH1(Pd—Ag)}$

Table S8.3: Donor–Acceptor Interactions in CMD Transition State **$1_{CH1(Pd—Ag)}$**. Important interactions are shown in bold font type and the corresponding natural bond orbitals are qualitatively represented in the immediately accompanying table given below

interacting partners	donor	acceptor	$E^{(2)}$ (in kcal/mol)
Ag–Pd	BD(1)Pd 13 - P 14	LP*(6)Ag 20	6.47
	BD(1)Pd 13 - P 14	LP*(7)Ag 20	8.95
	BD(1)Pd 13 - P 14	BD*(1)Ag 20 - P 25	2.73
	BD(1)Pd 13 - P 17	LP*(6)Ag 20	4.63
	BD(1)Pd 13 - P 17	LP*(7)Ag 20	7.54
	CR(1)Pd 13	LP*(7)Ag 20	6.48
	CR(1)Pd 13	BD*(1)Ag 20 - P 25	2.15

	BD(1)Ag 20 - P 25	LP*(5)Pd 13	2.76
	BD(1)Ag 20 - P 25	LP*(7)Pd 13	15.00
	BD(1)Ag 20 - P 25	BD*(1)Pd 13 - P 14	2.07
	BD(1)Ag 20 - P 25	BD*(1)Pd 13 - P 17	2.01
	CR(1)Ag 20	LP*(7)Pd 13	7.05
Pd–C	BD(1) C 1 - C 2	LP*(5)Pd 13	5.78
	BD(1) C 1 - C 2	LP*(6)Pd 13	4.12
	BD(1) C 1 - C 6	LP*(5)Pd 13	5.13
	BD(1) C 1 - C 6	LP*(6)Pd 13	2.53
	BD(1) C 1 - H 33	LP*(5)Pd 13	25.18
	BD(1) C 1 - H 33	LP*(6)Pd 13	13.63
	BD(1) C 1 - H 33	**BD*(1)Pd 13 - P 17**	**7.25**
	$\sigma_{C–H} \rightarrow \sigma^*_{Pd–P}$		
	CR(1) C 1	LP*(5)Pd 13	4.99
	CR(1) C 1	LP*(6)Pd 13	1.91
	LP(1) C 1	BD*(1)Pd 13 - P 14	1.64
	LP(1) C 1	**BD*(1)Pd 13 - P 17**	**15.27**
	$pz \rightarrow \sigma^*_{Pd–P}$		
	BD(1)Pd 13 - P 14	**LP(1) C 1**	**2.08**
	BD(1)Pd 13 - P 17	**LP(1) C 1**	**2.49**
	$\sigma_{Pd–P} \rightarrow pz$		
	CR(1)Pd 13	LP(1) C 1	3.83
	CR(4)Pd 13	LP(1) C 1	2.27
	LP(1)Pd 13	**LP(1) C 1**	**1.60**
	$dz^2 \rightarrow pz$		
C–H	BD(1) C 1 - H 33	BD*(1) C 1 - H 33	2.11
	LP(1) C 1	**BD*(1) C 1 - H 33**	**13.98**
	$pz \rightarrow \sigma^*_{C–H}$		

Table S8.4: Donor–Acceptor Interactions in CMD Transition State $\mathbf{1_{CH1(Pd)}}$. Important interactions are shown in bold font type and the corresponding natural bond orbitals are qualitatively represented in the immediately accompanying table given below

interacting partners	donor	acceptor	$E^{(2)}$ (in kcal/mol)
Pd–C	BD(1) C 8 - C 9	LP*(6)Pd 13	4.09
	BD(2) C 8 - C 9	LP*(6)Pd 13	3.33
	BD(2) C 8 - C 9	LP*(7)Pd 13	1.52
	BD(2) C 8 - C 9	BD*(1)Pd 13 - P 35	2.30
	BD(1) C 8 - H 28	LP*(5)Pd 13	17.19
	BD(1) C 8 - H 28	LP*(6)Pd 13	32.98
	BD(1) C 8 - H 28	**BD*(1)Pd 13 - P 35**	**10.05**
	$\sigma_{C–H} \rightarrow \sigma^*_{Pd–P}$		
	CR(1) C 8	LP*(5)Pd 13	1.61
	CR(1) C 8	LP*(6)Pd 13	4.11
	BD(1)Pd 13 - P 14	**BD*(1) C 8 - H 28**	**2.00**
	$dxy \rightarrow \sigma^*_{C–H}$		
	CR(1)Pd 13	BD*(2) C 8 - C 9	1.60
C–H	BD(2) C 8 - C 9	BD*(1) C 8 - H 28	8.75
	BD(1) C 8 - H 28	BD*(1) C 8 - H 28	2.57

Table S8.5: Electron Occupancies in Palladium d-orbitals in the RE Transition States

TS	orbitals involved	occupancy	relative occupancy	overall occupancy
$\mathbf{1_{RE1(Pd)}}$	d(xy)	1.740	0.000	9.192
	d(yz)	1.818		
	d(xz)	1.866		
	$d(x^2-y^2)$	1.845		
	$d(z^2)$	1.922		

$\mathbf{1}_{\mathbf{RE1(Pd—Ag)}}$	d(xy)	1.789	+0.049	9.382
	d(yz)	1.851	+0.033	
	d(xz)	1.945	+0.079	
	d(x^2-y^2)	1.945	+0.100	
	d(z^2)	1.858	+0.064	

The overall charge on the palladium center, in $\mathbf{1}_{\mathbf{RE1(Pd—Ag)}}$, suggests a relatively electron rich Pd in the heterobimetallic RE TS. This appears contrary to the general expectation that the metal center should remain electron deficient for a favorable reductive elimination.[22] Interestingly, there are experimental as well as theoretical studies that suggest alternative scenarios based on the nature of ligands bound to the palladium center.[23] It is proposed that (a) better the σ-donating ability of the leaving group, easier is the reductive elimination step, (b) stronger donor ligands *trans* to the leaving group leads to higher barrier for the elimination reaction. In another relatively simpler proposal, Hartwig suggested the use of charges on the complementary pairs of nucleophilic heteroatom-containing ligand and an electrophilic aryl ligand involved in the RE step.[21, 24] For instance, in the illustration given below for $\mathbf{1}_{\mathbf{RE1(Pd)}}$, the charges on C3 and P14 are critical to the RE step. We note that this analysis works well in our systems.

Reductive Elimination

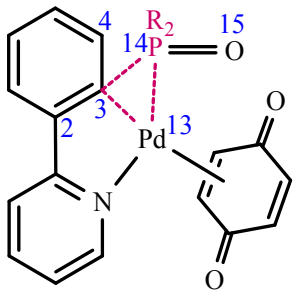

$\mathbf{1}_{\mathbf{RE1(Pd)}}$

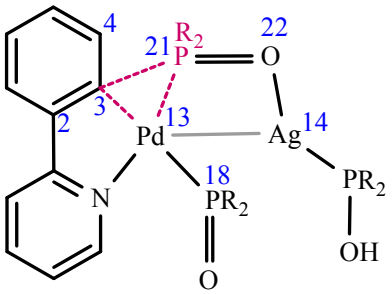

$\mathbf{1}_{\mathbf{RE1(Pd—Ag)}}$

[20] H. A. Brune, B. Stapp and G. Schmidtberg, *J. Organomet. Chem.* 1986, **307**, 129.
[21] (a) J. F Hartwig,. *Acc. Chem. Res.* 1998, **31,** 852. (b) K. Tatsumi, R. Hoffmann, A. Yamamoto and J. K Stille,. *Bull. Chem. Soc. Jpn.* 1981, **54**, 1857.
[22] G. Mann, D. Baranano, J. F. Hartwig, A. L. Rheingold and I. A. Guzei, *J. Am. Chem. Soc.* 1998, **120,** 9205.

Table S8.6: Comparison of the Electronic Charge on the reductively eliminating centers in the RE Transition States

TS	reductively eliminating center	charge on center	relative charges
$\mathbf{1}_{\mathbf{RE1(Pd)}}$	C3	-0.198	0.0
	P14	2.239	
$\mathbf{1}_{\mathbf{RE1(Pd—Ag)}}$	C3	-0.295	-0.097
	P21	2.220	-0.019

A relatively higher charge on the nucleophilic aryl carbon (C3 as shown above) of the reductively eliminating aryl ligand partner is noticed in the case of $\mathbf{1}_{\mathbf{RE1(Pd—Ag)}}$. Hence, we see a greater propensity towards reductive elimination, manifested as lower energy $\mathbf{1}_{\mathbf{RE1(Pd—Ag)}}$ as compared to $\mathbf{1}_{\mathbf{RE1(Pd)}}$. A closer inspection of the electron delocalization (as summarized in Table S7.11) revealed finer and interesting details. Since phosphorous is a good π-acceptor ligand capable of donation and back donation, it helps in increasing the electron density on palladium and the C3 center.

Table S8.7: Donor–Acceptor Interactions in RE Transition State $\mathbf{1}_{\mathbf{RE1(Pd—Ag)}}$. Important interactions are shown in bold font type and the corresponding natural bond orbitals are qualitatively represented in the immediately accompanying table given below

interacting partners	donor	acceptor	$E^{(2)}$ (in kcal/mol)
Ag–Pd	BD(1)Pd 13 - P 18	LP*(6)Ag 14	19.34
	BD(1)Pd 13 - P 18	LP*(7)Ag 14	18.85
	BD(1)Pd 13 - P 18	LP*(8)Ag 14	2.93
	CR(1)Pd 13	LP*(6)Ag 14	3.87
	CR(1)Pd 13	LP*(7)Ag 14	13.05
	LP(4)Pd 13	LP*(6)Ag 14	7.61
	LP(4)Pd 13	LP*(7)Ag 14	3.27
	LP(5)Pd 13	LP*(6)Ag 14	6.86

	LP(5)Pd 13	LP*(7)Ag 14	3.62
	CR(1)Ag 14	LP*(7)Pd 13	9.11
	CR(1)Ag 14	BD*(1)Pd 13 - P 18	7.99
Pd–C	BD(1) C 3 - C 4	LP*(6)Pd 13	8.26
	BD(2) C 3 - C 4	LP*(6)Pd 13	2.73
	BD(2) C 3 - C 4	LP*(8)Pd 13	4.21
	BD(2) C 3 - C 4	BD*(1)Pd 13 - P 18	1.65
	BD(1) C 3 - P 21	LP*(6)Pd 13	86.82
	CR(1) C 3	LP*(6)Pd 13	7.87
	CR(1)Pd 13	BD*(2) C 3 - C 4	3.55
	CR(4)Pd 13	BD*(1) C 3 - P 21	2.27
	LP(5)Pd 13	**BD*(2) C 3 - C 4**	**5.24**
	$dyz \rightarrow \pi^*_{C=C}$		
	LP(5)Pd 13	**BD*(1) C 3 - P 21**	**73.27**
	$dyz \rightarrow \sigma^*_{C-P}$		
	BD(1) C 3 - P 21	**BD*(1)Pd 13 - P 18**	**8.17**
	$\sigma_{C-P} \rightarrow \sigma^*_{Pd-P}$		
C–P	BD(1) C 3 - C 4	LP*(2) P 21	2.09
	BD(2) C 3 - C 4	LP*(1) P 21	7.41
	BD(2) C 3 - C 4	LP*(2) P 21	2.64
	BD(2) C 3 - C 4	BD*(1) C 3 - P 21	3.57
	BD(1) C 3 - P 21	BD*(1) P 21 - O 22	9.35
	CR(2) P 21	LP*(2) P 21	8.24
P–Pd	BD(1) P 21 - O 22	LP*(6)Pd 13	6.02
	CR(2) P 21	LP*(6)Pd 13	14.95
	CR(2) P 21	LP*(8)Pd 13	4.40
	BD(1)Pd 13 - P 18	LP*(1) P 21	4.86
	CR(1)Pd 13	LP*(1) P 21	5.23
	LP(2)Pd 13	**LP*(2) P 21**	**2.05**
	LP(3)Pd 13	**LP*(1) P 21**	**3.10**

	LP(5)Pd 13	**LP*(1) P 21**	**13.09**
	LP(5)Pd 13	**LP*(2) P 21**	**10.06**
	d → p		

Table S8.8: Donor–Acceptor Interactions in RE Transition State $\mathbf{1_{RE1(Pd)}}$. Important interactions are shown in bold font type and the corresponding natural bond orbitals are qualitatively represented in the immediately accompanying table given below

interacting partners	donor	acceptor	$E^{(2)}$ (in kcal/mol)
Pd–C	BD(1) C 3 - P 14	LP*(6)Pd 13	115.87
	BD(1) C 3 - P 14	LP*(7)Pd 13	22.08
	BD(1) C 3 - P 14	LP*(8)Pd 13	2.76
	CR(1) C 3	LP*(6)Pd 13	5.00
	CR(1) C 3	LP*(7)Pd 13	2.03
	CR(1) C 3	LP*(8)Pd 13	2.01
	CR(1)Pd 13	BD*(2) C 3 - C 4	2.62
	CR(4)Pd 13	BD*(1) C 3 - P 14	3.84
	CR(4)Pd 13	BD*(2) C 3 - C 4	1.64
	LP(4)Pd 13	**BD*(1) C 3 - P 14**	**49.30**
	dx^2-$y^2 \rightarrow \sigma^*_{C-P}$		
	LP(4)Pd 13	**BD*(2) C 3 - P 14**	**1.89**
	LP(5)Pd 13	**BD*(1) C 3 - P 14**	**32.71**
	$dxy \rightarrow \sigma^*_{C-P}$		
	LP(5)Pd 13	**BD*(2) C 3 - C 4**	**2.65**
	$dxy \rightarrow \pi^*_{C=C}$		
C–P	BD(2) C 3 - C 4	LP*(1) P 14	5.87
	BD(2) C 3 - C 4	BD*(1) C 3 - P 14	4.04
	BD(1) C 3 - P 14	LP*(1) P 14	3.99
	BD(1) C 3 - P 14	BD*(1) P 14 - O 15	6.73
	BD(1) P 14 - O 15	BD*(1) C 3 - P 14	3.86

	CR(2) P 14	BD*(1) C 3 - P 14	5.05
P–Pd	BD(1) P 14 - O 15	LP*(6)Pd 13	6.93
	BD(1) P 14 - O 15	LP*(7)Pd 13	1.95
	BD(1) P 14 - O 15	LP*(9)Pd 13	5.40
	CR(2) P 14	LP*(6)Pd 13	14.16
	CR(2) P 14	LP*(7)Pd 13	5.87
	CR(2) P 14	LP*(9)Pd 13	5.34
	CR(1)Pd 13	LP*(1) P 14	5.17
	LP(2)Pd 13	**LP*(2) P 14**	**1.82**
	LP(3)Pd 13	**LP*(2) P 14**	**4.95**
	LP(4)Pd 13	**LP*(1) P 14**	**1.64**
	d → p		
	LP(4)Pd 13	BD*(1) P 14 - O 15	3.13

Reaction 2

Table S8.9: Electron Occupancies in Palladium d-orbitals in the CMD Transition States

TS	orbitals involved	occupancy	relative occupancy	overall occupancy
2$_{CH1(Pd)}$	d(xy)	1.961	0.000	8.931
	d(yz)	1.971		
	d(xz)	1.963		
	d(x^2-y^2)	1.101		
	d(z^2)	1.935		
2$_{CH1(Pd—Ag)}$	d(xy)	1.921	-0.040	8.925
	d(yz)	1.943	-0.028	
	d(xz)	1.680	-0.283	
	d(x^2-y^2)	1.445	+0.344	

	d(z^2)	1.936	-0.001	

CMD

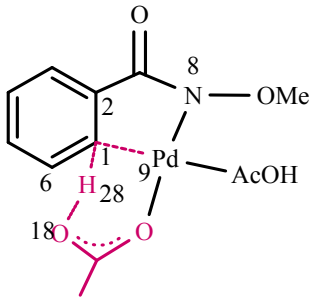

2$_{\mathbf{CH1(Pd)}}$

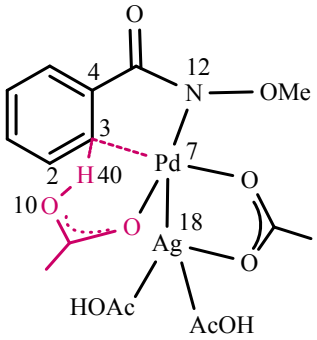

2$_{\mathbf{CH1(Pd–Ag)}}$

Table S8.10: Donor–Acceptor Interactions in CMD Transition State **2**$_{\mathbf{CH1(Pd—Ag)}}$. Important interactions are shown in bold font type and the corresponding natural bond orbitals are qualitatively represented in the immediately accompanying table given below

interacting partners	donor	acceptor	$E^{(2)}$ (in kcal/mol)
Ag–Pd	BD(1) C 3 -Pd 7	LP*(6)Ag 18	14.11
	BD(1) C 3 -Pd 7	LP*(7)Ag 18	6.83
	BD(1) C 3 -Pd 7	LP*(9)Ag 18	2.64
	BD(1)Pd 7 - N 12	LP*(6)Ag 18	14.60
	BD(1)Pd 7 - N 12	LP*(7)Ag 18	5.66
	BD(1)Pd 7 - N 12	LP*(9)Ag 18	4.32
	CR(1)Pd 7	LP*(7)Ag 18	7.01
	CR(1)Pd 7	LP*(9)Ag 18	1.12
	LP(2)Pd 7	LP*(6)Ag 18	2.23
	LP(4)Pd 7	LP*(6)Ag 18	3.90
	LP(4)Pd 7	LP*(7)Ag 18	1.66
	CR(1)Ag 18	LP*(7)Pd 7	6.80

	CR(1)Ag 18	BD*(1) C 3 -Pd 7	1.61
	CR(1)Ag 18	BD*(1)Pd 7 - N 12	2.60
	CR(2)Ag 18	LP*(7)Pd 7	1.42
	LP(5)Ag 18	LP*(7)Pd 7	1.72
Pd–C	BD(1) C 2 - C 3	LP*(5)Pd 7	1.02
	BD(1) C 2 - C 3	LP*(6)Pd 7	1.38
	BD(1) C 2 - C 3	**BD*(1)Pd 7 - N 12**	**1.37**
	$\sigma_{C\text{-}C} \rightarrow \sigma^*_{Pd\text{-}N}$		
	BD(1) C 3 - C 4	LP*(6)Pd 7	1.65
	BD(1) C 3 -Pd 7	LP*(5)Pd 7	1.10
	BD(1) C 3 -Pd 7	BD*(1) C 3 -Pd 7	6.04
	BD(1) C 3 -Pd 7	**BD*(1)Pd 7 - N 12**	**51.80**
	$\sigma_{C\text{-}Pd} \rightarrow \sigma^*_{Pd\text{-}N}$		
	CR(1) C 3	LP*(6)Pd 7	1.55
	CR(1)Pd 7	BD*(1) C 3 -Pd 7	2.11
	CR(2)Pd 7	BD*(1)Pd 7 - N 12	1.54
	CR(3)Pd 7	BD*(1) C 3 -Pd 7	3.32
	CR(4)Pd 7	LP*(7)Pd 7	1.06
	CR(4)Pd 7	BD*(1)Pd 7 - N 12	1.30
	LP(1) C 3	LP*(7)Pd 7	1.52
	LP(1) C 3	**BD*(1) C 3 -Pd 7**	**4.89**
	$pz \rightarrow \sigma^*_{C\text{-}Pd}$		

Table S8.11: Donor–Acceptor Interactions in CMD Transition State $\mathbf{2_{CH1(Pd)}}$. Important interactions are shown in bold font type and the corresponding natural bond orbitals are qualitatively represented in the immediately accompanying table given below

interacting partners	donor	acceptor	$E^{(2)}$ (in kcal/mol)

Pd–C	BD(1) C 1 - C 2	LP*(6)Pd 9	2.81
	BD(2) C 1 - C 2	BD*(1) C 1 -Pd 9	61.90
	BD(2) C 1 - C 2	BD*(1) N 8 -Pd 9	4.00
	BD(1) C 1 - C 6	LP*(6)Pd 9	2.44
	BD(1) C 1 - C 6	BD*(1) C 1 -Pd 9	3.23
	BD(1) C 1 -Pd 9	LP*(6)Pd 9	5.13
	BD(1) C 1 -Pd 9	LP*(7)Pd 9	13.29
	BD(1) C 1 -Pd 9	BD*(2) C 1 - C 2	456.40
	BD(1) C 1 -Pd 9	BD*(1) C 1 - C 6	6.15
	BD(1) C 1 -Pd 9	BD*(1) C 1 -Pd 9	145.56
	BD(1) C 1 -Pd 9	**BD*(1) C 1 - H 28**	**129.26**
	$\sigma_{C–Pd} \rightarrow \sigma^*_{C–H}$		
	BD(1) C 1 -Pd 9	BD*(1) N 8 -Pd 9	391.02
	BD(1) C 1 - H 28	LP*(5)Pd 9	8.19
	BD(1) C 1 - H 28	LP*(6)Pd 9	20.69
	BD(1) C 1 - H 28	LP*(7)Pd 9	31.17
	BD(1) C 1 - H 28	**BD*(1) N 8 -Pd 9**	**42.96**
	$\sigma_{C–H} \rightarrow \sigma^*_{Pd–N}$		
	BD(1) N 8 -Pd 9	BD*(1) C 1 -Pd 9	12.87
	CR(1) C 1	LP*(6)Pd 9	2.89
	CR(1)Pd 9	BD*(1) C 1 -Pd 9	1.64
	CR(2)Pd 9	BD*(1) C 1 -Pd 9	3.92
C–H	BD(1) C 1 - H 28	BD*(1) C 1 - C 2	4.97
	BD(1) C 1 - H 28	BD*(2) C 1 - C 2	705.90
	BD(1) C 1 - H 28	BD*(1) C 1 - C 6	4.14
	BD(1) C 1 - H 28	**BD*(1) C 1 -Pd 9**	**366.85**
	$\sigma_{C–H} \rightarrow \sigma^*_{C-Pd}$		
	BD(1) C 1 - H 28	BD*(1) C 1 - H 28	119.65

Table S8.12: Electron Occupancies in Palladium d-orbitals in the RE Transition States

TS	orbitals involved	occupancy	relative occupancy	overall occupancy
2$_{\mathbf{RE1(Pd)}}$	d(xy)	1.779	0.000	8.913
	d(yz)	1.647		
	d(xz)	1.864		
	d(x^2-y^2)	1.789		
	d(z^2)	1.834		
2$_{\mathbf{RE1(Pd—Ag)}}$	d(xy)	1.937	+0.158	8.870
	d(yz)	1.417	-0.230	
	d(xz)	1.972	+0.108	
	d(x^2-y^2)	1.701	-0.088	
	d(z^2)	1.843	-0.009	

Reductive Elimination

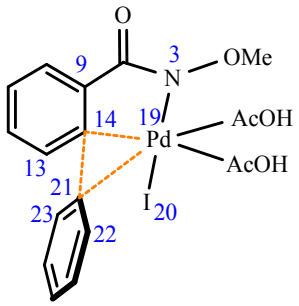

2$_{\mathbf{RE1(Pd)}}$

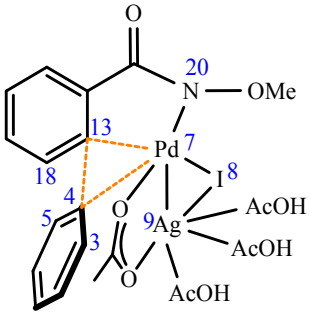

2$_{\mathbf{RE1(Pd–Ag)}}$

Table S8.13: Comparison of the Electronic Charge on the reductively eliminating centers in the RE Transition States

TS	reductively eliminating center	charge on center	relative charges
2RE1$_{\mathbf{(Pd)}}$	C14	-0.028	0.000

	C21	-0.042	
2RE1$_{(Pd—Ag)}$	C13	-0.031	-0.003
	C4	0.009	+0.051

Table S8.14: Donor–Acceptor Interactions in RE Transition State **2$_{RE1(Pd—Ag)}$**. Important interactions are shown in bold font type and the corresponding natural bond orbitals are qualitatively represented in the immediately accompanying table given below

interacting partners	donor	acceptor	$E^{(2)}$ (in kcal/mol)
Ag–Pd	BD(1)Pd 7 - I 8	LP*(6)Ag 9	34.87
	BD(1)Pd 7 - I 8	LP*(7)Ag 9	9.85
	BD(1)Pd 7 - I 8	LP*(8)Ag 9	4.10
	BD(1)Pd 7 - I 8	LP*(9)Ag 9	1.78
	BD(1)Pd 7 - C 13	LP*(6)Ag 9	3.99
	BD(1)Pd 7 - C 13	LP*(8)Ag 9	4.96
	BD(1)Pd 7 - C 13	LP*(9)Ag 9	3.10
	BD(1)Pd 7 - N 20	LP*(6)Ag 9	8.92
	BD(1)Pd 7 - N 20	LP*(8)Ag 9	4.78
	BD(1)Pd 7 - N 20	LP*(9)Ag 9	5.71
	CR(1)Pd 7	LP*(6)Ag 9	9.00
	CR(1)Pd 7	LP*(7)Ag 9	1.09
	CR(1)Pd 7	LP*(8)Ag 9	7.84
	CR(1)Pd 7	LP*(9)Ag 9	3.02
	CR(1)Ag 9	LP*(6)Pd 7	5.48
	CR(1)Ag 9	BD*(1)Pd 7 - I 8	5.38
	CR(1)Ag 9	BD*(1)Pd 7 - N 20	1.63
	LP(5)Ag 9	BD*(1)Pd 7 - I 8	2.51
Pd–$C_{substrate}$	BD(1)Pd 7 - I 8	BD*(1)Pd 7 - C 13	3.43
	BD(1)Pd 7 - C 13	BD*(1)Pd 7 - I 8	18.07
	BD(1)Pd 7 - C 13	BD*(1)Pd 7 - C 13	13.84

	BD(1)Pd 7 - C 13	**BD*(1)Pd 7 - N 20**	**34.97**
	$\sigma_{C\text{-}Pd} \rightarrow \sigma^*_{Pd\text{-}N}$		
	BD(1)Pd 7 - N 20	BD*(1)Pd 7 - C 13	34.42
	BD(1) C 13 - C 14	BD*(1)Pd 7 - C 13	2.22
	BD(1) C 13 - C 14	BD*(1)Pd 7 - N 20	1.71
	BD(1) C 13 - C 18	LP*(5)Pd 7	1.36
	BD(1) C 13 - C 18	BD*(1)Pd 7 - C 13	2.14
	BD(1) C 13 - C 18	BD*(1)Pd 7 - N 20	1.54
	BD(2) C 13 - C 18	LP*(6)Pd 7	1.99
	CR(2)Pd 7	BD*(1)Pd 7 - C 13	2.57
	CR(3)Pd 7	BD*(1)Pd 7 - C 13	1.48
	LP(3)Pd 7	**BD*(2) C 13 - C 18**	**1.92**
	$dxy \rightarrow \pi^*_{C=C}$		
	LP(4)Pd 7	BD*(2) C 13 - C 18	1.20
C_{aryl}–$C_{substrate}$	BD(2) C 4 - C 5	BD*(2) C 13 - C 18	3.36
	BD(1) C 13 - C 18	LP*(1) C 4	1.22
	BD(2) C 13 - C 18	LP*(1) C 4	41.45
	BD(2) C 13 - C 18	BD*(2) C 4 - C 5	3.81
C_{aryl}–Pd	BD(1) C 3 - C 4	LP*(6)Pd 7	7.67
	BD(1) C 3 - C 4	BD*(1)Pd 7 - C 13	1.73
	BD(1) C 4 - C 5	LP*(6)Pd 7	7.60
	BD(1) C 4 - C 5	BD*(1)Pd 7 - C 13	1.44
	BD(2) C 4 - C 5	LP*(6)Pd 7	5.29
	CR(1) C 4	LP*(6)Pd 7	4.88
	CR(1) C 4	BD*(1)Pd 7 - C 13	1.57
	BD(1)Pd 7 - C 13	**LP*(1) C 4**	**346.28**
	$\sigma_{C\text{-}Pd} \rightarrow py_{C(aryl)}$		
	BD(1)Pd 7 - N 20	LP*(1) C 4	4.40
	CR(1)Pd 7	LP*(1) C 4	9.74
	CR(2)Pd 7	LP*(1) C 4	8.12

	CR(2)Pd 7	BD*(2) C 4 - C 5	1.28
	LP(3)Pd 7	LP*(1) C 4	4.05
	LP(4)Pd 7	**LP*(1) C 4**	**111.87**
	dx^2-y^2 → $px_{C(aryl)}$		
	LP(4)Pd 7	BD*(2) C 4 - C 5	3.89

Table S8.15: Donor–Acceptor Interactions in RE Transition State $\mathbf{2_{RE1(Pd)}}$. Important interactions are shown in bold font type and the corresponding natural bond orbitals are qualitatively represented in the immediately accompanying table given below

interacting partners	donor	acceptor	$E^{(2)}$ (in kcal/mol)
Pd–$C_{substrate}$	BD(1) C 9 - C 14	LP*(5)Pd 19	3.99
	BD(1) C 9 - C 14	LP*(6)Pd 19	8.79
	BD(1) C 9 - C 14	LP*(7)Pd 19	4.50
	BD(2) C 9 - C 14	LP*(5)Pd 19	2.59
	BD(2) C 9 - C 14	LP*(7)Pd 19	4.01
	BD(2) C 9 - C 14	BD(2) C 9 - C 14	3.22
	BD(1) C 13 - C 14	LP*(5)Pd 19	2.15
	BD(1) C 13 - C 14	LP*(6)Pd 19	6.62
	BD(1) C 13 - C 14	LP*(7)Pd 19	3.17
	BD(1) C 14 - C 21	LP*(5)Pd 19	37.28
	BD(1) C 14 - C 21	LP*(6)Pd 19	44.10
	BD(1) C 14 - C 21	**BD*(1) N 3 -Pd 19**	**25.36**
	$\sigma_{C–C} \rightarrow \sigma^*_{N\text{-}Pd}$		
	BD(1) C 14 - C 21	BD*(1)Pd 19 - I 20	1.39
	BD(1) C 21 - C 22	LP*(5)Pd 19	2.52
	BD(1) C 21 - C 22	LP*(6)Pd 19	8.20
	BD(1) C 21 - C 22	LP*(7)Pd 19	1.71
	CR(1) C 14	LP*(5)Pd 19	2.16
	CR(1) C 14	LP*(6)Pd 19	7.03

	CR(1) C 14	LP*(7)Pd 19	2.74
	CR(1)Pd 19	BD*(2) C 9 - C 14	2.67
	CR(1)Pd 19	BD*(1) C 13 - C 14	1.00
	CR(3)Pd 19	BD*(1) C 14 - C 21	3.13
	CR(4)Pd 19	BD*(1) C 14 - C 21	1.63
	LP(4)Pd 19	BD*(2) C 9 - C 14	5.92
	LP(4)Pd 19	**BD*(1) C 14 - C 21**	**59.65**
	dxz → $\sigma^*_{C–C}$		
C_{aryl}–$C_{substrate}$	BD(2) C 9 - C 14	BD*(1) C 14 - C 21	2.27
	BD(1) C 9 - C 10	BD*(1) C 14 - C 21	4.05
	BD(2) C 9 - C 14	BD*(2) C 21 - C 23	1.36
	BD(2) C 21 - C 23	BD*(2) C 9 - C 14	3.58
	BD(2) C 21 - C 23	BD*(1) C 14 - C 21	2.40
	CR(1) C 14	BD*(1) C 14 - C 21	3.80
	CR(1) C 21	BD*(1) C 14 - C 21	4.28
C_{aryl}–Pd	BD(1) C 21 - C 23	LP*(5)Pd 19	2.06
	BD(1) C 21 - C 23	LP*(6)Pd 19	7.71
	BD(1) C 21 - C 23	LP*(7)Pd 19	2.09
	BD(2) C 21 - C 23	LP*(5)Pd 19	3.91
	BD(2) C 21 - C 23	LP*(7)Pd 19	4.10
	BD(2) C 21 - C 23	BD*(1) N 3 -Pd 19	1.29
	CR(1)Pd 19	BD*(2) C 21 - C 23	2.49
	CR(1) C 21	LP*(5)Pd 19	1.97
	CR(1) C 21	LP*(6)Pd 19	7.26
	CR(1) C 21	LP*(7)Pd 19	1.20
	LP(4)Pd 19	**BD*(2) C 21 - C 23**	**6.50**
	dxz → $\pi^*_{C=C}$		

Reaction 3

Table S8.16: Electron Occupancies in Palladium d-orbitals in the CMD Transition States

TS	orbitals involved	occupancy	relative occupancy	overall occupancy
3$_{\mathbf{CH1(Pd)}}$	d(xy)	1.534	0.000	8.881
	d(yz)	1.934		
	d(xz)	1.927		
	d(x^2-y^2)	1.532		
	d(z^2)	1.953		
3$_{\mathbf{CH1(Pd—Ag)}}$	d(xy)	1.958	+0.424	8.892
	d(yz)	1.810	-0.124	
	d(xz)	1.966	+0.039	
	d(x^2-y^2)	1.698	+0.166	
	d(z^2)	1.459	-0.494	

CMD

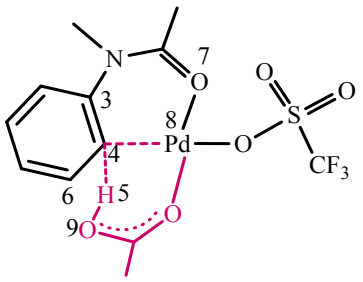

3$_{\mathbf{CH1(Pd)}}$

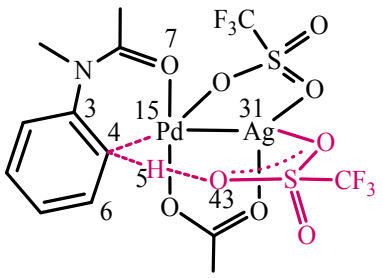

3$_{\mathbf{CH1(Pd—Ag)}}$

Table S8.17: Donor–Acceptor Interactions in CMD Transition State **3**$_{\mathbf{CH1(Pd—Ag)}}$. Important interactions are shown in bold font type and the corresponding natural bond orbitals are qualitatively represented in the immediately accompanying table given below

interacting	donor	acceptor	$E^{(2)}$ (in

partners			kcal/mol)
Ag–Pd	CR(1)Ag 31	LP*(5)Pd 15	5.30
	CR(1)Ag 31	LP*(6)Pd 15	1.86
	CR(1)Ag 31	LP*(8)Pd 15	4.18
	LP(5)Ag 31	LP*(5)Pd 15	2.09
	LP(5)Ag 31	LP*(8)Pd 15	1.36
Pd–C	**BD(1) C 4 - H 5**	**LP*(5)Pd 15**	**3.76**
	$\sigma_{C–H} \rightarrow dz^2$		
	BD(1) C 4 - H 5	LP*(6)Pd 15	4.35
	BD(1) C 4 - H 5	LP*(8)Pd 15	1.76
	BD(1) C 4 - C 6	LP*(5)Pd 15	1.80
	BD(1) C 4 - C 6	LP*(6)Pd 15	4.28
	CR(1) C 4	LP*(6)Pd 15	4.59
	CR(1)Pd 15	BD*(1) C 4 -Pd 15	8.38
	CR(2)Pd 15	BD*(1) C 4 -Pd 15	6.41
	LP(3)Pd 15	**BD*(1) C 3 - C 4**	**1.22**
	$dxz \rightarrow \sigma^*_{C–C}$		
	LP(4)Pd 15	**BD*(1) C 4 -Pd 15**	**1.64**
	$dxy \rightarrow \sigma^*_{C–Pd}$		
C–H	**BD(1) C 4 -Pd 15**	**BD*(1) C 4 - H 5**	**2.45**
	$dx^2\text{-}y^2 \rightarrow \sigma^*_{C–H}$		
	BD(1) C 4 - C 6	BD*(1) C 4 - H 5	1.26

Table S8.18: Donor–Acceptor Interactions in CMD Transition State $\mathbf{3_{CH1(Pd)}}$. Important interactions are shown in bold font type and the corresponding natural bond orbitals are qualitatively represented in the immediately accompanying table given below

interacting partners	donor	acceptor	$E^{(2)}$ (in kcal/mol)
Pd–C	**BD(2) C 3 - C 4**	**BD*(1) C 4 -Pd 8**	**134.28**

	$\pi_{C=C} \rightarrow \sigma^*_{C–Pd}$		
	BD(1) C 4 - C 6	LP*(6)Pd 8	3.32
	CR(1) C 4	BD(1) C 4 -Pd 8	4.61
	CR(1) C 4	LP*(6)Pd 8	3.60
	CR(1) C 4	BD*(1) C 4 -Pd 8	2.38
	CR(1)Pd 8	BD*(1) C 4 -Pd 8	4.95
	CR(2)Pd 8	BD*(1) C 4 -Pd 8	3.03
	LP(4)Pd 8	**BD*(1) C 4 -Pd 8**	**1.63**
	$dxz \rightarrow \sigma^*_{C–Pd}$		
C–H	**BD(1) C 4 -Pd 8**	**BD*(1) C 4 - H 5**	**75.35**
	$\sigma_{C–Pd} \rightarrow \sigma^*_{C–H}$		
	BD(2) C 3 - C 4	BD*(1) C 4 - H 5	35.79

Table S8.19: Electron Occupancies in Palladium d-orbitals in the Oxidative Addition Transition States

TS	orbitals involved	occupancy	relative occupancy	overall occupancy
$3_{OA(Pd)}$	d(xy)	1.954	0.000	8.881
	d(yz)	1.790		
	d(xz)	1.890		
	$d(x^2-y^2)$	1.537		
	$d(z^2)$	1.708		
$3_{OA(Pd—Ag)}$	d(xy)	1.691	-0.263	8.882
	d(yz)	1.900	+0.110	
	d(xz)	1.867	-0.023	
	$d(x^2-y^2)$	1.768	+0.231	
	$d(z^2)$	1.6550	-0.053	

Oxidative Addition

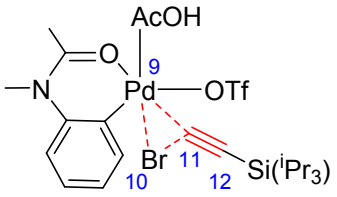

3$_{\mathbf{OA(Pd)}}$

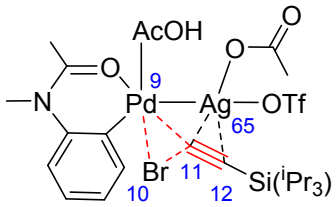

3$_{\mathbf{OA(Pd—Ag)}}$

Table S8.20: Donor–Acceptor Interactions in Oxidative Addition Transition State **3**$_{\mathbf{OA(Pd—Ag)}}$. Important interactions are shown in bold font type and the corresponding natural bond orbitals are qualitatively represented in the immediately accompanying table given below

interacting partners	donor	acceptor	$E^{(2)}$ (in kcal/mol)
Ag–Pd	BD (1) C 6 -Pd 9	LP*(7)Ag 65	2.80
	CR (1)Pd 9	LP*(6)Ag 65	4.40
	CR (1)Pd 9	LP*(7)Ag 65	13.88
	CR (1)Pd 9	LP*(9)Ag 65	2.39
	CR (1)Ag 65	LP*(8)Pd 9	4.97
Pd–C	CR (1)Pd 9	BD*(1) C 11 - C 12	2.94
	CR (1)Pd 9	BD*(3) C 11 - C 12	6.22
	CR (2)Pd 9	BD*(3) C 11 - C 12	1.02
	CR (3)Pd 9	BD*(3) C 11 - C 12	3.28
	LP (3)Pd 9	BD*(2) C 11 - C 12	4.97
	LP (4)Pd 9	BD*(3) C 11 - C 12	11.40
	BD (1) C 11 - C 12	LP*(5)Pd 9	4.74
	BD (1) C 11 - C 12	LP*(6)Pd 9	8.27
	BD (1) C 11 - C 12	LP*(8)Pd 9	3.92
	BD (3) C 11 - C 12	LP*(5)Pd 9	12.18
	BD (3) C 11 - C 12	LP*(6)Pd 9	7.34
	BD (3) C 11 - C 12	LP*(8)Pd 9	10.94
Pd-Br	CR (3)Pd 9	BD*(1)Br 10 - C 11	1.51

	LP (4)Pd 9	BD*(1)Br 10 - C 11	28.24
	BD (1)Br 10 - C 11	LP*(5)Pd 9	24.84
	BD (1)Br 10 - C 11	LP*(6)Pd 9	37.31
	LP (3)Br 10	LP*(5)Pd	10.14
	LP (3)Br 10	LP*(6)Pd	11.50
	LP (3)Br 10	LP*(8)Pd	7.00
C-Br	LP (1)Br 10	BD*(2) C 11 - C 12	2.07
	LP (1)Br 10	BD*(3) C 11 - C 12	4.13
	LP (2)Br 10	BD*(2) C 11 - C 12	1.60
	LP (2)Br 10	BD*(3) C 11 - C 12	3.84

Table S8.21: Donor–Acceptor Interactions in Oxidative Addition Transition State $\mathbf{3_{OA(Pd)}}$. Important interactions are shown in bold font type and the corresponding natural bond orbitals are qualitatively represented in the immediately accompanying table given below

interacting partners	donor	acceptor	$E^{(2)}$ (in kcal/mol)
Pd–C	CR (1)Pd 9	BD*(1) C 11 - C 12	3.17
	CR (1)Pd 9	BD*(3) C 11 - C 12	2.44
	LP (3)Pd 9	BD*(2) C 11 - C 12	4.71
Pd-Br	LP (1)Br 10	LP*(6)Pd 9	2.27
	LP (2)Br 10	LP*(5)Pd 9	6.65
	LP (3)Br 10	LP*(5)Pd 9	9.79
C-Br	LP (1)Br 10	BD*(2) C 11 - C 12	3.22
	LP (2)Br 10	BD*(3) C 11 - C 12	7.04

Table S8.22: Electron Occupancies in Palladium d-orbitals in the RE Transition States

TS	orbitals involved	occupancy	relative occupancy	overall occupancy
$\mathbf{3_{RE1(Pd)}}$	d(xy)	1.890	0.000	8.783

	d(yz)	1.672		
	d(xz)	1.955		
	d(x^2-y^2)	1.626		
	d(z^2)	1.639		
3$_{\mathbf{RE1(Pd—Ag)}}$	d(xy)	1.748	-0.142	8.767
	d(yz)	1.489	-0.183	
	d(xz)	1.863	-0.092	
	d(x^2-y^2)	1.814	+0.188	
	d(z^2)	1.852	+0.213	

Reductive Elimination

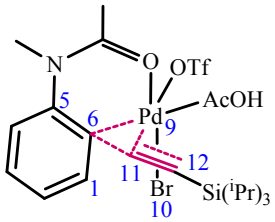

3$_{\mathbf{RE1(Pd)}}$

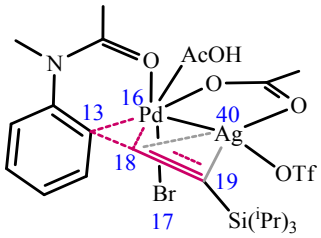

3$_{\mathbf{RE1(Pd—Ag)}}$

Table S8.23: Comparison of the Electronic Charge on the reductively eliminating centers in the RE Transition States

TS	reductively eliminating center	charge on center	relative charges
3$_{\mathbf{RE1(Pd)}}$	C6	-0.014	0.0
	C11	-0.075	
3$_{\mathbf{RE1(Pd—Ag)}}$	C13	-0.022	-0.008
	C18	-0.159	-0.084

Table S8.24: Donor–Acceptor Interactions in RE Transition State **3**$_{\mathbf{RE1(Pd—Ag)}}$. Important interactions are shown in bold font type and the corresponding natural bond orbitals are qualitatively represented in the immediately accompanying table given below

interacting partners	donor	acceptor	$E^{(2)}$ (in kcal/mol)
Ag–Pd	BD(1) C 13 -Pd 16	LP*(6)Ag 40	15.23
	BD(1) C 13 -Pd 16	LP*(7)Ag 40	9.53
	BD(1) C 13 -Pd 16	LP*(8)Ag 40	3.77
	BD(1)Pd 16 -Br 17	LP*(6)Ag 40	6.42
	BD(1)Pd 16 -Br 17	LP*(7)Ag 40	6.46
	BD(1)Pd 16 -Br 17	LP*(8)Ag 40	1.57
	BD(1)Pd 16 - C 18	LP*(6)Ag 40	21.16
	BD(1)Pd 16 - C 18	LP*(7)Ag 40	12.72
	BD(1)Pd 16 - C 18	LP*(8)Ag 40	6.78
Pd–C_{aryl}	BD(1) C 8 - C 13	LP*(4)Pd 16	2.35
	BD(1) C 8 - C 13	LP*(6)Pd 16	5.37
	BD(2) C 8 - C 13	LP*(6)Pd 16	2.86
	BD(1) C 13 -Pd 16	LP*(4)Pd 16	3.28
	BD(1) C 13 -Pd 16	**BD*(1)Pd 16 -Br 17**	**83.61**
	$\sigma_{C\text{-}Pd} \rightarrow \sigma^*_{Pd\text{–}Br}$		
	BD(1) C 13 -Pd 16	**BD*(1)Pd 16 - C 18**	**148.54**
	$\sigma_{C\text{-}Pd} \rightarrow \sigma^*_{Pd\text{–}C}$		
	BD(1)Pd 16 -Br 17	BD*(1) C 13 -Pd 16	20.07
	BD(1)Pd 16 -Br 17	BD*(1)Pd 16 - C 18	30.56
	BD(1)Pd 16 -Br 17	BD*(2) C 18 - C 19	2.01
C_{aryl}–C	BD(1) C 13 -Pd 16	BD*(3) C 18 - C 19	11.22
	BD(3) C 18 - C 19	BD*(2) C 8 - C 13	4.00
	BD(3) C 18 - C 19	BD*(1) C 13 -Pd 16	4.01
C–Pd	**BD(1) C 18 - C 19**	**LP*(4)Pd 16**	**5.46**
	$\sigma_{C\text{-}C} \rightarrow dxz$		
	BD(1) C 18 - C 19	LP*(6)Pd 16	1.47
	BD(1) C 18 - C 19	BD*(1)Pd 16 - C 18	4.62
	BD(1) C 18 - C 19	BD*(1)Pd 16 -Br 17	1.82

	BD(2) C 18 - C 19	LP*(4)Pd 16	4.30
	BD(2) C 18 - C 19	LP*(5)Pd 16	1.83
	BD(3) C 18 - C 19	LP*(6)Pd 16	3.41

Table S8.25: Donor–Acceptor Interactions in RE Transition State $\mathbf{3_{RE1(Pd)}}$. Important interactions are shown in bold font type and the corresponding natural bond orbitals are qualitatively represented in the immediately accompanying table given below

interacting partners	donor	acceptor	$E^{(2)}$ (in kcal/mol)
Pd–C_{aryl}	BD(1) C 1 - C 6	LP*(4)Pd 9	2.59
	BD(1) C 1 - C 6	LP*(6)Pd 9	4.06
	BD(2) C 1 - C 6	BD*(1)Pd 9 - C 11	1.17
	BD(1) C 5 - C 6	LP*(4)Pd 9	3.88
	BD(1) C 5 - C 6	LP*(6)Pd 9	3.88
	BD(1) C 6 -Pd 9	LP*(4)Pd 9	2.35
	BD(1) C 6 -Pd 9	BD*(1) C 6 -Pd 9	33.96
	BD(1) C 6 -Pd 9	**BD*(1)Pd 9 -Br 10**	**77.81**
	$\sigma_{C\text{-}Pd} \rightarrow \sigma^*_{Pd\text{-}Br}$		
	BD(1)Pd 9 -Br 10	BD*(1) C 6 -Pd 9	19.77
C_{aryl}–C_{alkyne}	BD(2) C 1 - C 6	BD*(3) C 11 - C 12	5.85
	BD(1) C 5 - C 6	BD*(3) C 11 - C 12	1.55
	BD(1) C 6 -Pd 9	BD*(1) C 11 - C 12	1.33
	BD(3) C 11 - C 12	BD*(2) C 1 - C 6	7.44
	BD(3) C 11 - C 12	BD*(1) C 6 -Pd 9	4.51
C_{alkyne}–Pd	**BD(1) C 6 -Pd 9**	**BD*(1)Pd 9 - C 11**	**143.73**
	$\sigma_{C\text{-}Pd} \rightarrow \sigma^*_{Pd\text{-}C}$		
	BD(1) C 6 -Pd 9	BD*(3) C 11 - C 12	7.34
	BD(1)Pd 9 -Br 10	BD*(1)Pd 9 - C 11	27.37
	BD(1)Pd 9 -Br 10	BD*(2) C 11 - C 12	1.65
	BD(1)Pd 9 - C 11	**BD*(1) C 6 -Pd 9**	**107.94**

	$\sigma_{C\text{-}Pd} \rightarrow \sigma^*_{Pd\text{-}C}$		
	BD(1)Pd 9 - C 11	BD*(1)Pd 9 -Br 10	74.42
	BD(2) C 11 - C 12	LP*(4)Pd 9	1.31
	BD(2) C 11 - C 12	LP*(5)Pd 9	1.31

Table S8.26: Electron Occupancies in Palladium d-orbitals in the CMD Transition States

TS	orbitals involved	occupancy	relative occupancy	overall occupancy
4$_{\mathbf{CH1(Pd)}}$	d(xy)	1.872	0.000	9.122
	d(yz)	1.748		
	d(xz)	1.790		
	d(x^2-y^2)	1.856		
	d(z^2)	1.855		
4$_{\mathbf{CH1(Pd—Ag)}}$	d(xy)	1.841	-0.031	9.124
	d(yz)	1.936	+0.188	
	d(xz)	1.590	-0.200	
	d(x^2-y^2)	1.849	-0.007	
	d(z^2)	1.908	+0.053	

CMD

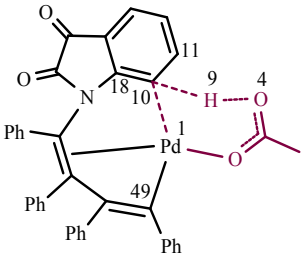

4$_{\mathbf{CH1(Pd)}}$

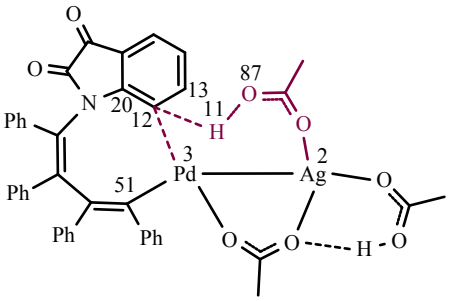

4$_{\mathbf{CH1(Pd—Ag)}}$

Table S8.27: Donor–Acceptor Interactions in CMD Transition State $\mathbf{4_{CH1(Pd—Ag)}}$. Important interactions are shown in bold font type and the corresponding natural bond orbitals are qualitatively represented in the immediately accompanying table given below

interacting partners	donor	acceptor	$E^{(2)}$ (in kcal/mol)
Ag–Pd	BD(1)Pd 3 - C 51	LP*(6)Ag 2	2.44
	BD(1)Pd 3 - C 51	LP*(7)Ag 2	1.77
	CR(1)Pd 3	LP*(6)Ag 2	8.80
	CR(1)Pd 3	LP*(7)Ag 2	7.58
	LP(3)Pd 3	LP*(6)Ag 2	2.04
	CR(1)Ag 2	LP*(5)Pd 3	7.70
	CR(1)Ag 2	LP*(6)Pd 3	11.93
	LP(5)Ag 2	LP*(5)Pd 3	1.80
Pd–C	BD(1) C 12 - C 13	LP*(5)Pd 3	2.53
	BD(1) C 12 - C 13	LP*(7)Pd 3	2.75
	BD(1) C 12 - C 20	LP*(5)Pd 3	2.33
	BD(1) C 12 - C 20	LP*(7)Pd 3	3.70
	BD(1) H 11 - C 12	**BD*(1)Pd 3 - C 51**	**7.67**
	$\sigma_{C–H} \rightarrow \sigma^*_{Pd-C}$		
	BD(1) H 11 - C 12	LP*(5)Pd 3	21.52
	BD(1) H 11 - C 12	LP*(7)Pd 3	7.02
	CR(1)Pd 3	LP(1) C 12	4.93
	CR(2)Pd 3	LP(1) C 12	1.63
	CR(1) C 12	LP*(5)Pd 3	1.59
	CR(1) C 12	LP*(7)Pd 3	2.54
	LP(4)Pd 3	**LP(1) C 12**	**4.69**
	$dx^2\text{-}y^2 \rightarrow py$		
	LP(1) C 12	LP*(5)Pd 3	28.59
	LP(1) C 12	LP*(6)Pd 3	1.67

	LP(1) C 12	LP*(7)Pd 3	2.97
	LP(1) C 12	**BD*(1)Pd 3 - C 51**	**73.46**
	py → σ^*_{Pd-C}		
C–H	**LP(1) C 12**	**BD*(1) H 11 - C 12**	**16.27**
	pz → $\sigma^*_{C–H}$		

Table S8.28: Donor–Acceptor Interactions in CMD Transition State $\mathbf{4_{CH1(Pd)}}$. Important interactions are shown in bold font type and the corresponding natural bond orbitals are qualitatively represented in the immediately accompanying table given below

interacting partners	donor	acceptor	$E^{(2)}$ (in kcal/mol)
Pd–C	**BD(1)Pd 1 - C 49**	**BD*(2) C 10 - C 11**	**1.42**
	$\sigma_{C–Pd} \rightarrow \pi^*_{C=C}$		
	BD(1) H 9 - C 10	LP*(5)Pd 1	12.24
	BD(1) H 9 - C 10	LP*(6)Pd 1	32.18
	BD(1) H 9 - C 10	LP*(8)Pd 1	1.15
	BD(1) H 9 - C 10	**BD*(1)Pd 1 - C 49**	**9.28**
	$\sigma_{C–H} \rightarrow \sigma^*_{Pd-C}$		
	BD(1) C 10 - C 11	LP*(6)Pd 1	4.62
	BD(2) C 10 - C 11	LP*(5)Pd 1	4.20
	BD(2) C 10 - C 11	LP*(6)Pd 1	4.15
	BD(2) C 10 - C 11	**BD*(1)Pd 1 - C 49**	**3.33**
	$\pi_{C=C} \rightarrow \sigma^*_{Pd-C}$		
	BD(1) C 10 - C 18	LP*(6)Pd 1	6.18
	LP(2)Pd 1	BD*(2) C 10 - C 11	1.83
C–H	BD(2) C 10 - C 11	BD*(1) H 9 - C 10	9.87
	BD(1) H 9 - C 10	BD*(1) H 9 - C 10	2.32

Table S8.29: Electron Occupancies in Palladium d-orbitals in the RE Transition States

TS	orbitals involved	occupancy	relative occupancy	overall occupancy
4$_{\mathbf{RE1(Pd)}}$	d(xy)	1.950	0.000	9.313
	d(yz)	1.804		
	d(xz)	1.894		
	d(x^2-y^2)	1.731		
	d(z^2)	1.934		
4$_{\mathbf{RE1(Pd—Ag)}}$	d(xy)	1.917	-0.033	9.261
	d(yz)	1.929	+0.125	
	d(xz)	1.809	-0.085	
	d(x^2-y^2)	1.701	-0.003	
	d(z^2)	1.897	-0.037	

Reductive Elimination

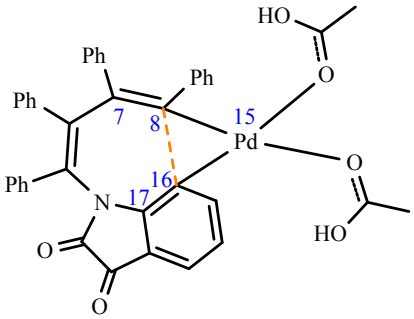

4$_{\mathbf{RE1(Pd)}}$

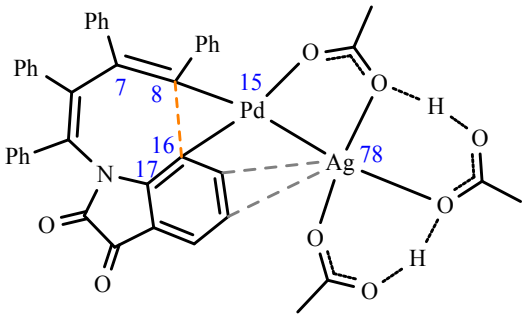

4$_{\mathbf{RE1(Pd—Ag)}}$

Table S8.30: Comparison of the Electronic Charge on the reductively eliminating centers in the RE Transition States

TS	reductively eliminating center	charge on center	relative charges
4$_{\mathbf{RE1(Pd)}}$	C8	-0.112	0.000
	C16	-0.235	

$4_{RE1(Pd—Ag)}$	C8	-0.083	+0.029
	C16	-0.155	+0.080

Table S8.31: Donor–Acceptor Interactions in RE Transition State $4_{RE1(Pd—Ag)}$. Important interactions are shown in bold font type and the corresponding natural bond orbitals are qualitatively represented in the immediately accompanying table given below

interacting partners	donor	acceptor	$E^{(2)}$ (in kcal/mol)
Ag–Pd	CR(1)Pd 15	LP*(6)Ag 78	15.52
	CR(1)Pd 15	LP*(7)Ag 78	12.02
	LP(4)Pd 15	LP*(6)Ag 78	6.08
	LP(4)Pd 15	LP*(7)Ag 78	2.16
	LP(3)Pd 15	LP*(6)Ag 78	0.84
	LP(3)Pd 15	LP*(7)Ag 78	0.69
	CR(1)Ag 78	LP*(6)Pd 15	8.39
	CR(1)Ag 78	LP*(7)Pd 15	9.57
	LP(5)Ag 78	LP*(6)Pd 15	0.93
Pd–C_{alkyne}	CR(1)Pd 15	BD*(2) C 7 - C 8	2.03
	CR(2)Pd 15	BD*(1) C 8 - C 16	3.27
	CR(3)Pd 15	BD*(1) C 8 - C 16	1.57
	LP(2)Pd 15	BD*(1) C 7 - C 8	1.09
	LP(2)Pd 15	BD*(1) C 8 - C 9	1.17
	LP(4)Pd 15	BD*(2) C 7 - C 8	2.36
	LP(5)Pd 15	BD*(2) C 7 - C 8	5.48
	LP(5)Pd 15	**BD*(1) C 8 - C 16**	**104.52**
	dx^2-y^2 → $\sigma^*_{C(alkyne)–C(isatin)}$		
C_{alkyne}–C_{isatin}	BD(2) C 7 - C 8	BD*(1) C 8 - C 16	3.92
	BD(2) C 16 - C 17	BD*(2) C 7 - C 8	2.58
	BD(2) C 16 - C 17	BD*(1) C 8 - C 16	5.23
C_{isatin}–Pd	CR(1)Pd 15	BD*(2) C 16 - C 17	2.51

	CR(2)Pd 15	BD*(2) C 16 - C 17	1.75
	LP(5)Pd 15	**BD*(2) C 16 - C 17**	**7.06**
	dx^2-y^2 → $\pi^*_{C=C}$		
	LP(4)Pd 15	BD*(2) C 16 - C 17	2.17

Table S8.32: Donor–Acceptor Interactions in RE Transition State **$4_{RE1(Pd—Ag)}$**. Important interactions are shown in bold font type and the corresponding natural bond orbitals are qualitatively represented in the immediately accompanying table given below

interacting partners	donor	acceptor	$E^{(2)}$ (in kcal/mol)
Pd–C_{alkyne}	CR(1)Pd 15	BD*(2) C 7 - C 8	3.16
	CR(2)Pd 15	BD*(1) C 8 - C 16	1.84
	CR(3)Pd 15	BD*(1) C 8 - C 16	2.01
	LP(5)Pd 15	BD*(2) C 7 - C 8	10.29
	LP(5)Pd 15	**BD*(1) C 8 - C 16**	**64.02**
	dx^2-y^2 → $\sigma^*_{C(alkyne)–C(isatin)}$		
	LP(4)Pd 15	BD*(2) C 7 - C 8	1.45
C_{alkyne}–C_{isatin}	BD(1) C 8 - C 9	BD*(2) C 16 - C 17	1.50
	BD(1) C 8 - C 16	BD*(2) C 16 - C 17	0.92
	BD(1) C 16 - C 17	BD*(2) C 7 - C 8	1.40
	BD(1) C 16 - C 17	BD*(1) C 16 - C 21	2.83
	BD(2) C 16 - C 17	BD*(2) C 7 - C 8	5.01
	BD(2) C 16 - C 17	BD*(1) C 8 - C 16	5.56
C_{isatin}–Pd	LP(4)Pd 15	BD*(2) C 16 - C 17	1.20
	LP(5)Pd 15	**BD*(2) C 16 - C 17**	**11.47**
	dxz → $\pi^*_{C=C}$		

8.3: (C) Charges on Important Atoms Involved in the CMD Transition States

Reaction 1

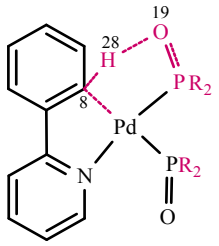

1$_{\mathbf{CH1(Pd)}}$

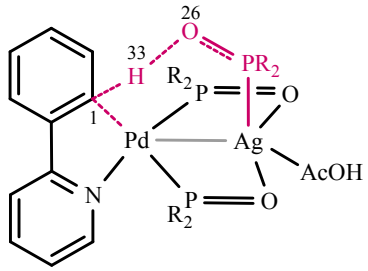

1$_{\mathbf{CH1(Pd—Ag)}}$

Table S8.33: NPA Charges on Atoms Involved in the CMD Transition States for Reaction **1**

TS	atom	charge on center	relative charge on center
1$_{\mathbf{CH1(Pd)}}$	C8	-0.414	0.000
	H28	0.437	
	O19	-1.085	
1$_{\mathbf{CH1(Pd—Ag)}}$	C1	-0.436	-0.022
	H33	0.441	+0.004
	O26	-1.082	-0.003

Reaction 2

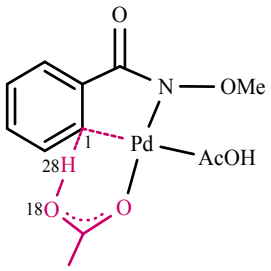

2$_{\mathbf{CH1(Pd)}}$

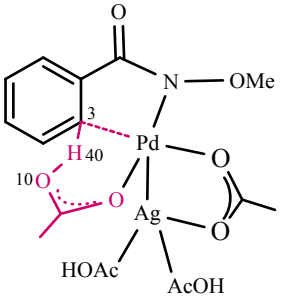

2$_{\mathbf{CH1(Pd–Ag)}}$

Table S8.34: NPA Charges on Atoms Involved in the CMD Transition States for Reaction **2**

TS	atom	charge on center	Relative charge on center
2$_{\mathbf{CH1(Pd)}}$	C1	-0.374	0.000
	H28	0.404	
	O18	-0.720	
2$_{\mathbf{CH1(Pd—Ag)}}$	C3	-0.356	+0.018
	H40	0.405	+0.001
	O10	-0.726	-0.006

Reaction 3

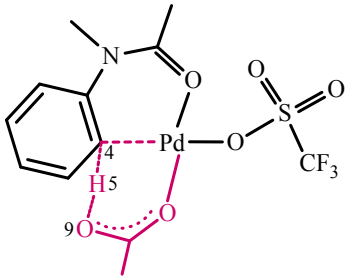

3$_{\mathbf{CH1(Pd)}}$

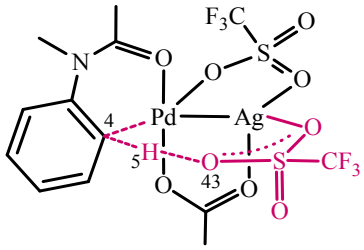

3$_{\mathbf{CH1(Pd—Ag)}}$

Table S8.35: NPA Charges on Atoms Involved in the CMD Transition States for Reaction **3**

TS	atom	charge on center	relative charge on center
3$_{\mathbf{CH1(Pd)}}$	C4	-0.415	0.000
	H5	0.398	
	O9	-0.689	
3$_{\mathbf{CH1(Pd—Ag)}}$	C4	-0.430	-0.015
	H5	0.452	+0.054
	O43	-0.964	-0.275

Reaction 4

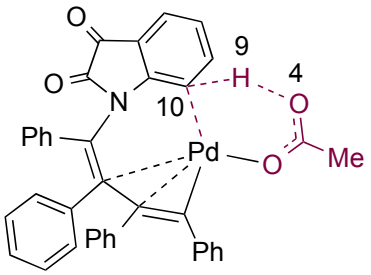

4$_{\mathbf{CH1(Pd)}}$

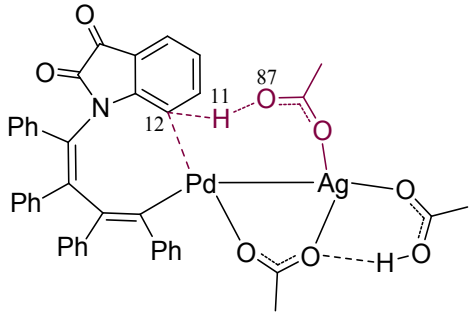

4$_{\mathbf{CH1(Pd—Ag)}}$

Table S8.36: NPA Charges on Atoms Involved in the CMD Transition States for Reaction **4**

TS	atom	charge on center	relative charge on center
4$_{\mathbf{CH1(Pd)}}$	C10	-0.479	0.000
	H9	0.430	
	O4	-0.738	
4$_{\mathbf{CH1(Pd—Ag)}}$	C12	-0.513	-0.034
	H11	0.434	+0.004
	O87	-0.742	-0.004

In all these transition states, the positive charge n the proton being activated is larger in the case of bimetallic transition state as compared to the monometallic analogue. In general, the carbon that forms the palladacycle shows an increased negative charge in the bimetallic transition state.

Section 9

AIM Analysis

For a detailed description of AIM computations, see Section 1(C).

All values of ρ and ∇^2 are in atomic units multiplied by 10^{-2}

Pd-Ag BCP

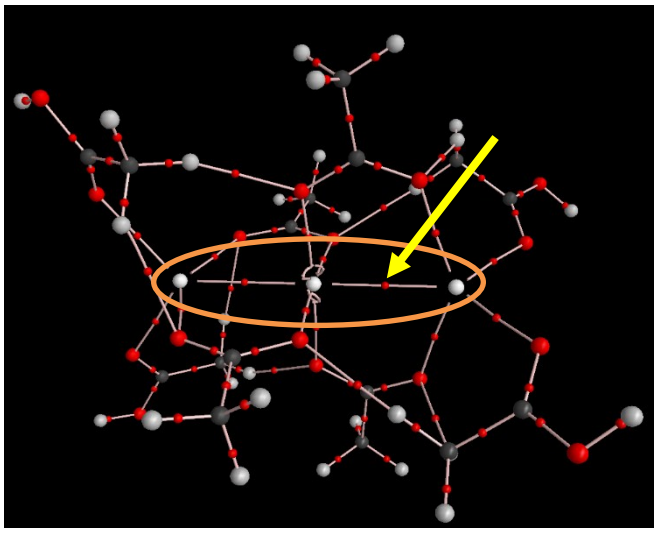

ρ	∇^2
2.68	-2.42

Figure S9.1: Identification of Pd-Ag bond critical points at the M06/6-31G**(LANL2DZ=Pd, Ag) level of theory using the geometry as noted in the crystal structure obtained from the CCDC.[25]

Topology map of electron densities of CMD and RE transition states with Pd-Ag species. The Pd-Ag region is encircled.

25. Kozitsyna, N. Y.; Nefedov, S. E.; Klyagina, A. P.; Markov, A. A.; Dobrokhotova, Z. V.; Velikodny,Y. A.; Kochubey, D. I.; Zyubina, T. S.; Gekhman, A. E.; Vargaftik, M. N.; Moiseev, I. I. *Inorg. Chim. Acta.* **2011**, *370*, 382.

3$_{\mathbf{CH1(Pd–Ag)}}$ **3**$_{\mathbf{RE1(Pd–Ag)}}$

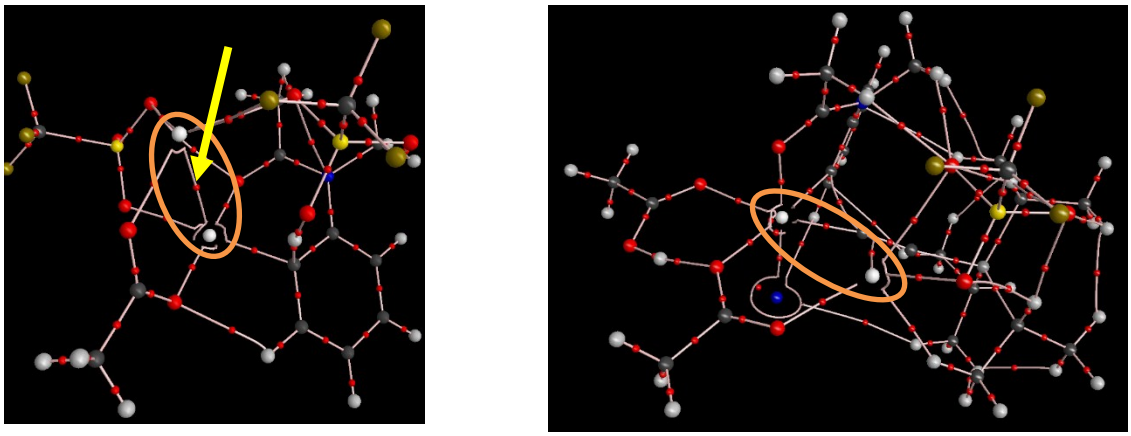

ρ	∇^2	ρ	∇^2
2.41	-2.04	No bcp	No bcp

Figure S9.2: AIM topological map of CMD and RE transition states for reaction-**3.**

4$_{\mathbf{CH1(Pd–Ag)}}$ **4**$_{\mathbf{RE1(Pd–Ag)}}$

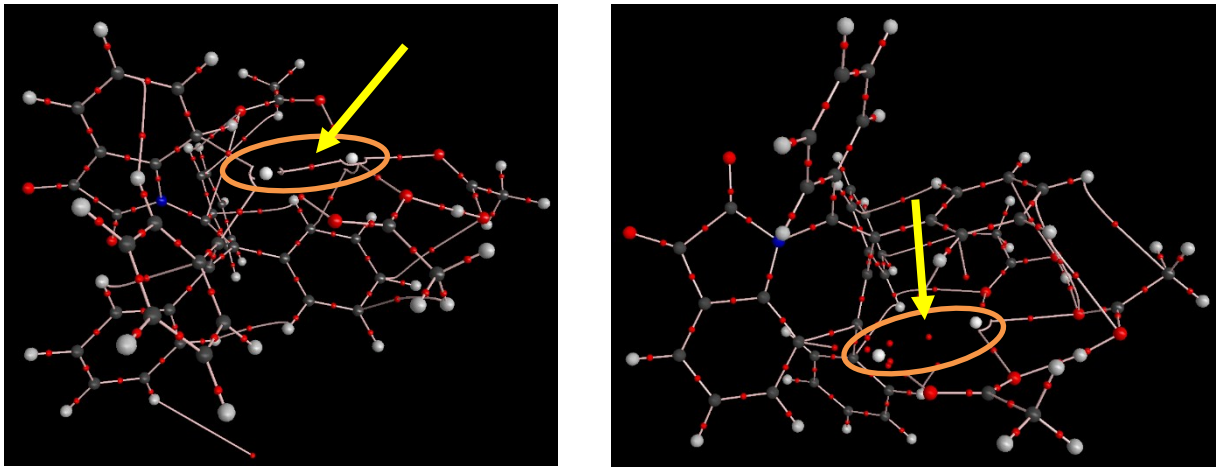

ρ	∇^2	ρ	∇^2
2.44	-2.03	2.98	-2.34

Figure S9.3: AIM topological map of CMD and RE transition states for reaction-**4.**

Table S9.1: AIM parameters obtained using the wave function generated at the SMD$_{(solvent)}$/M06/6-31G**,LANL2DZ(Pd,Ag,Br,I) level of theory for all the transition states

	ρ	∇^2	G	$1/4*\nabla^2$	$H=1/4\nabla^2-G$	V=H-G
1$_{\mathbf{CH1(Pd–Ag)}}$	0.01595	-0.00946	0.00968	-0.00237	**-0.01204**	-0.02172
1$_{\mathbf{RE1(Pd–Ag)}}$	0.03551	-0.02582	0.02929	-0.00646	**-0.03574**	-0.06503
2$_{\mathbf{CH1(Pd–Ag)}}$	0.02834	-0.02565	0.02643	-0.00641	**-0.03285**	-0.05928
2$_{\mathbf{RE1(Pd–Ag)}}$	No bcp					
3$_{\mathbf{CH1(Pd–Ag)}}$	0.02417	-0.02046	0.02054	-0.00512	**-0.02565**	-0.04619
3$_{\mathbf{RE1(Pd–Ag)}}$	No bcp					
4$_{\mathbf{CH1(Pd–Ag)}}$	0.02447	-0.02032	0.02058	-0.00508	**-0.02566**	-0.04625
4$_{\mathbf{RE1(Pd–Ag)}}$	0.02982	-0.02341	0.02520	-0.00585	**-0.03105**	-0.05626

Section 10

Kohn-Sham Molecular Orbital Analysis

Reaction: **1**

Total number of doubly occupied molecular orbitals in CMD transition state = 161

Total number of doubly occupied molecular orbitals in RE transition state = 144

(The preferred ligands around the metal centers need not remain identical in CMD and RE transition states (See Figure 2(a) and (b) in the main manuscript). It is important to note that the lowest energy transition states in each case were identified by invoking a large number of ligand exchange possibilities (e.g., Section 6)

CMD ($1_{CH1(Pd-Ag)}$)		**RE ($1_{RE1(Pd-Ag)}$)**	
Pd	HOMO-24	**Pd**	HOMO-24
d-orbital	coefficient	d-orbital	coefficient
d_{z2}	-0.00662	d_{z2}	-0.02348
d_{xz}	0.03566	d_{xz}	0.01231
d_{yz}	-0.03750	d_{yz}	0.02388
d_{xy}	0.12455	d_{xy}	-0.06435
d_{x2-y2}	-0.10540	d_{x2-y2}	-0.10720
Ag		**Ag**	
d_{z2}	-0.11415	d_{z2}	0.12971
d_{xz}	-0.16626	d_{xz}	0.10169
d_{yz}	0.00148	d_{yz}	0.24292
d_{xy}	0.13877	d_{xy}	0.19234
d_{x2-y2}	-0.16652	d_{x2-y2}	-0.08754

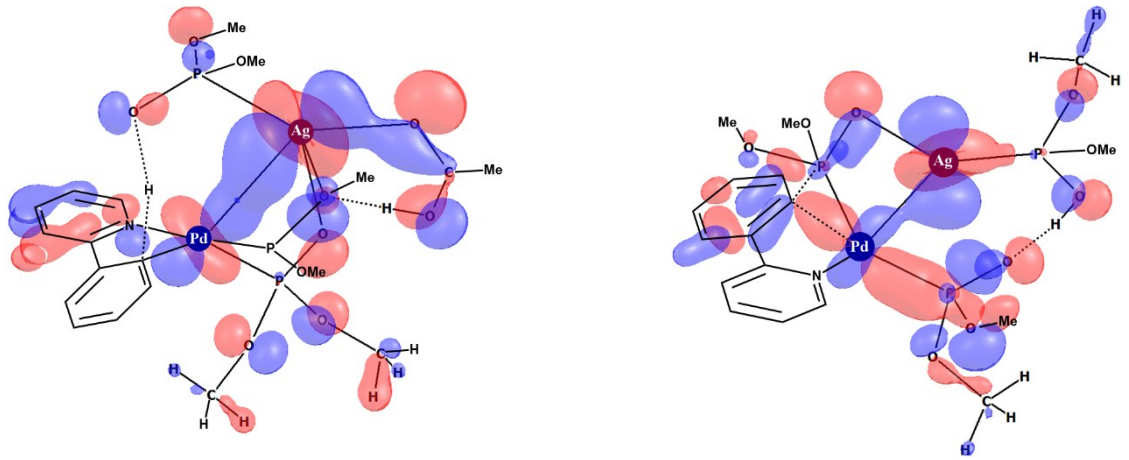

Figure S10.1: Kohn-Sham orbitals (contour value = 0.03) in the most preferred CMD and RE transition states for the phosphorylation reaction **1.**

In CMD TS, d_{xy}/d_{x2-y2} (Pd) interacts with d_{xz}/d_{x2-y2} (Ag). In RE TS, d_{x2-y2}(Pd) interacts with d_{yz}(Ag).